NIKHEF 96-031
PSI-PR-96-41

The fermion-loop scheme for finite-width effects in e^+e^- annihilation into four fermions

Wim Beenakker, Geert Jan van Oldenborgh
Instituut–Lorentz, Rijksuniversiteit Leiden, the Netherlands
Ansgar Denner
Paul-Scherrer-Institut, Würenlingen und Villigen, Switzerland
Stefan Dittmaier
Institut für Theoretische Physik, Universität Bielefeld, Germany
Jiri Hoogland
NIKHEF-H, Amsterdam, the Netherlands
Ronald Kleiss
University of Nijmegen, Nijmegen, the Netherlands
Costas G. Papadopoulos
Institute of Nuclear Physics, NRCPS Δημόκριτος, Athens, Greece
Giampiero Passarino
Dipartimento di Fisica Teorica, Università di Torino, Italy
INFN, Sezione di Torino, Italy

Abstract
We describe the gauge-invariant treatment of the finite-width effects of W and Z bosons in the fermion-loop scheme and its application to the six-fermion (LEP2) processes $e^-e^+ \to$ four fermions, with massless external fermions. The fermion-loop scheme consists in including all fermionic one-loop corrections in tree-level amplitudes and resumming the self-energies. We give explicit results for the unrenormalized fermionic one-loop contributions to the gauge-boson self-energies and the triple gauge-boson vertices, and perform the renormalization in a gauge-invariant way by introducing complex pole positions and running couplings. A simple effective Born prescription is presented, which allows for a relatively straightforward implementation of the fermion-loop scheme in LEP1 and LEP2 processes. We apply this prescription to typical LEP2 processes, i.e., $e^-e^+ \to \mu^-\bar{\nu}_\mu u\bar{d}$, $e^-e^+ \to s\bar{c}u\bar{d}$, and $e^-e^+ \to e^-\bar{\nu}_e u\bar{d}$, and give numerical comparisons with other gauge-invariance-preserving schemes in the energy range of LEP2, NLC and beyond.

1 Introduction

The incorporation of finite-width effects in the theoretical predictions for LEP2 processes and their implementation in the corresponding event generators necessitate a careful treatment. Independently of how finite widths of propagating particles are introduced, this requires (or at least mimics) a resummation of the vacuum-polarization effects. However, thereby the principle of gauge invariance must not be violated, i.e., the Ward identities have to be preserved; otherwise theoretical uncertainties may get out of control.

In a previous article [1] we discussed several schemes that allow the incorporation of finite-width effects in tree-level amplitudes without spoiling gauge invariance. We argued that the preferable (fermion-loop) scheme consists in the resummation of the fermionic one-loop corrections to the vector-boson propagators and the inclusion of all remaining fermionic one-loop corrections, in particular those to the Yang–Mills vertices. This resummation of one-particle-irreducible (1PI) fermionic $\mathcal{O}(\alpha)$ corrections involves the closed set of all $\mathcal{O}\left([N_c^f \alpha/\pi]^i\right)$ (leading color-factor) corrections, and is as such manifestly gauge-invariant. These corrections constitute the bulk of the width effects for gauge bosons and an important part of the complete set of weak corrections.

In Ref. [1] our main incentive was the discussion of the process $e^-e^+ \to e^-\bar{\nu}_e u\bar{d}$ at small scattering angles and LEP2 energies. Naive inclusion of the finite W-boson width breaks U(1) electromagnetic gauge invariance and leads to a totally wrong cross-section in the collinear limit, as e.g. discussed in Ref. [2]. By taking into account in addition the imaginary parts arising from cutting the massless fermion loops in the triple-gauge-boson vertex, U(1) gauge invariance is restored and a sensible cross-section is obtained.

After introducing the full fermion-loop (FL) scheme we restricted the explicit discussion in Ref. [1] to the minimal set of terms that are necessary to solve the U(1) problem in $e^-e^+ \to e^-\bar{\nu}_e u\bar{d}$, namely the imaginary parts of the contributions of massless fermions. In this paper we give the details of the full-fledged fermion-loop scheme, taking into account the complete fermionic one-loop corrections including all real and imaginary parts, and all contributions of the massive top quark. We perform a proper treatment of the neutral gauge-boson propagators by solving the Dyson equations for the photon, Z-boson, and mixed photon–Z propagators. This is necessary to guarantee the unitarity cancellations at high energies. The top-quark contributions are particularly important for delayed-unitarity effects. In this respect also terms involving the totally-antisymmetric ε-tensor (originating from vertex corrections) are relevant. While such terms are absent for complete generations of massless fermions owing to the anomaly cancellations, they show up for finite fermion masses. As the ε-dependent terms satisfy the Ward identities by themselves, they can be left out in more minimal treatments like the one used in Ref. [1].

We formulate a renormalization of the fermion-loop corrections using the language of running couplings. We show how to rewrite bare amplitudes in terms of these renormalized couplings and demonstrate that the resulting renormalized amplitudes respect gauge invariance, i.e., that they fulfill the relevant Ward

identities. Moreover, we give the explicit analytical results for the fermionic one-loop contributions to the gauge-boson self-energies and the triple gauge-boson vertices, which represent the necessary ingredients for applying the FL scheme to LEP2 processes with massless external fermions, i.e., $e^-e^+ \to 4f$.

The purpose of this paper is twofold. On the one hand it provides the justification of the FL scheme: we show that it is fully consistent, i.e., it is gauge-invariant, respects all relevant Ward identities, and describes the finite-width effects correctly. The full FL scheme includes the gauge-invariant subset of all one-loop fermionic corrections. However, our studies reveal that only relatively simple subsets of the fermionic corrections are required to arrive at a consistent description of finite-width effects for tree-level calculations. On the other hand the full FL scheme is also a starting point for the calculation of the $\mathcal{O}(\alpha)$ corrections to six-fermion processes. It includes all fermionic corrections and might therefore be used as a first approximation of the corrected cross-sections. However, very often our experience has shown, especially at LEP1, that bosonic corrections may become sizeable and comparable to the fermionic ones [3]. A large part of the bosonic corrections, as e.g. the leading-logarithmic corrections, factorize and can be treated by a convolution. Nevertheless the remaining bosonic corrections can still be non-negligible, i.e., of the order of one percent at LEP2 [4] and even larger at higher energies [5]. For the bosonic corrections a gauge-invariant treatment similar to the FL scheme, i.e., a Dyson summation without violating Ward identities, can be performed within the background-field method [6]. However, the resulting matrix elements are gauge-parameter-dependent at the loop level that is not completely taken into account.

The outline of the article is as follows: In Section 2 we describe the renormalization procedure and present the renormalized, resummed amplitudes for LEP1 processes, i.e., the four-fermion processes $e^+e^- \to f\bar{f}$ with massless external fermions. In Section 3 we discuss the fermionic one-loop corrections to the triple gauge-boson vertex and construct, from a set of basic matrix elements, the renormalized, resummed amplitudes for LEP2 processes, i.e., the six-fermion processes $e^-e^+ \to 4f$ with massless external fermions. By explicitly checking the relevant Ward identities, we verify the gauge invariance of these amplitudes. Using the processes $e^-e^+ \to \mu^-\bar{\nu}_\mu u\bar{d}$, $e^-e^+ \to s\bar{c}u\bar{d}$, and $e^-e^+ \to e^-\bar{\nu}_e u\bar{d}$ as examples, we give a numerical comparison with other schemes and show the numerical relevance of the resummed fermionic corrections at LEP2 energies and beyond in Section 4. Finally, a conclusion and outlook are given. In the appendices we give supplementary explicit formulae.

2 Renormalization

In this section we address the issue of how to define the renormalization, while at the same time performing a resummation of 1PI fermionic $\mathcal{O}(\alpha)$ corrections. In order to keep the expressions as compact as possible we renormalize the gauge-boson masses at their (gauge-invariant) complex pole [7]. This so-called "complex" scheme is also favored from a theoretical point of view [8]. It should

be noted, however, that the real part of the complex pole differs only by terms of order Γ^2/M^2 from the gauge-boson mass in the more familiar "LEP1" scheme, which is defined as the zero in the real part of the inverse gauge-boson propagator. As a result of the smallness of the decay widths of the gauge bosons this difference is marginal. In fact, all expressions in this section can also be computed using the LEP1 language, for which the FL scheme works equivalently well (see App. D). The computation of the renormalized parameters in the complex renormalization scheme is discussed in App. C.

Starting from the bare resummed propagators, the renormalization can be performed by first introducing renormalized masses and by subsequently rewriting all bare couplings in terms of running ones. The so-obtained renormalized resummed gauge-boson propagators automatically combine with the fermion–gauge-boson vertex functions to form dressed Born matrix elements, involving running couplings and propagator functions. This appealing feature is exemplified by the LEP1 processes, i.e., $e^+e^- \to f\bar{f}$ with massless external fermions.

2.1 Resumming the propagators

The natural way to incorporate the running-width effects of weak vector bosons is the resummation of the corresponding self-energy corrections. In the following we consider only fermionic one-loop corrections. As the on-shell widths of the W and Z bosons are entirely determined by fermionic decays, and the fermionic corrections are separately gauge-invariant and manifestly gauge-independent, this is a sensible approach. Solving the Dyson equations for the photon, Z, W, and mixed photon–Z propagators, one finds the following expressions for the transverse parts of the dressed propagators

$$
\begin{aligned}
\hat{P}_\gamma(p^2) &= \frac{p^2 - \hat{\mu}_Z + \hat{\Sigma}_Z(p^2)}{\left[p^2 + \hat{\Sigma}_\gamma(p^2)\right]\left[p^2 - \hat{\mu}_Z + \hat{\Sigma}_Z(p^2)\right] - \left[\hat{\Sigma}_X(p^2)\right]^2}\,, \\
\hat{P}_X(p^2) &= \frac{-\hat{\Sigma}_X(p^2)}{\left[p^2 + \hat{\Sigma}_\gamma(p^2)\right]\left[p^2 - \hat{\mu}_Z + \hat{\Sigma}_Z(p^2)\right] - \left[\hat{\Sigma}_X(p^2)\right]^2}\,, \\
\hat{P}_Z(p^2) &= \frac{p^2 + \hat{\Sigma}_\gamma(p^2)}{\left[p^2 + \hat{\Sigma}_\gamma(p^2)\right]\left[p^2 - \hat{\mu}_Z + \hat{\Sigma}_Z(p^2)\right] - \left[\hat{\Sigma}_X(p^2)\right]^2}\,, \\
\hat{P}_W(p^2) &= \frac{1}{p^2 - \hat{\mu}_W + \hat{\Sigma}_W(p^2)}\,,
\end{aligned}
\tag{1}
$$

where X denotes the photon–Z mixing, and $\hat{\mu}_Z$ and $\hat{\mu}_W$ represent the gauge-boson masses squared. Here and in the following, all parameters with a hat represent bare parameters. Functions with a hat depend on bare parameters. As the top-quark mass appears in the considered processes only at the one-loop level we need not explicitly distinguish between the bare and the renormalized top-quark masses. All other fermion masses are neglected whenever possible.

The self-energies $\hat{\Sigma}_i(p^2)$, with $i = Z, W$, are split into two pieces:

$$\hat{\Sigma}_Z(p^2) = \hat{\overline{\Sigma}}_Z(p^2) + \frac{\hat{g}_w^2}{\hat{c}_w^2}\, T_Z(p^2) \,,$$
$$\hat{\Sigma}_W(p^2) = \hat{\overline{\Sigma}}_W(p^2) + \hat{g}_w^2\, T_W(p^2) \,, \tag{2}$$

with $\hat{c}_w^2 \equiv 1 - \hat{s}_w^2 \equiv \hat{\mu}_W/\hat{\mu}_Z$, $\hat{g}_w^2 \equiv \hat{e}^2/(2\hat{s}_w^2)$, and $\hat{e}$ is the bare electromagnetic coupling. The first terms contain the universal contributions that have the structure of the photon self-energy, the second terms contain extra contributions that depend on the fermion masses and vanish with vanishing m_f. The dominant contributions to T_Z and T_W originate from the top quark. The explicit form of the self-energies can be found in App. A. We use the Feynman rules of Ref. [9].

As can be inferred from the explicit expressions, the universal parts of the self-energies are related as follows:

$$\hat{\overline{\Sigma}}_Z(p^2) \;=\; \frac{\hat{c}_w^2 - \hat{s}_w^2}{\hat{c}_w^2}\, \hat{\overline{\Sigma}}_W(p^2) + \frac{\hat{s}_w^2}{\hat{c}_w^2}\, \hat{\Sigma}_\gamma(p^2) \,,$$
$$\hat{\Sigma}_X(p^2) \;=\; -\frac{\hat{s}_w}{\hat{c}_w} \left[\hat{\overline{\Sigma}}_W(p^2) - \hat{\Sigma}_\gamma(p^2)\right] \,. \tag{3}$$

These relations are in fact a consequence of gauge invariance.

2.2 Definition of renormalized parameters

The W and Z bosons are renormalized at their *complex* pole[1]. In this "complex" scheme the renormalized complex squared masses $\mu_{W,Z}$ of the W and Z bosons are defined by

$$\hat{\mu}_W \;=\; \mu_W + \hat{\Sigma}_W(\mu_W) \,, \tag{4}$$
$$\hat{\mu}_Z \;=\; \mu_Z + \hat{Z}(\mu_Z) \,, \tag{5}$$

with

$$\hat{Z}(p^2) = \hat{\Sigma}_Z(p^2) - \frac{\hat{\Sigma}_X^2(p^2)}{p^2 + \hat{\Sigma}_\gamma(p^2)} \,. \tag{6}$$

After mass renormalization, i.e., insertion of Eqs.(4–5), the resummed propagators in Eq.(1) can be rewritten as

$$\hat{P}_\gamma(p^2) \;=\; \left[\frac{p^2}{p^2 + \hat{\Sigma}_\gamma(p^2)}\right] \frac{1}{p^2} + \left[\frac{\hat{\Sigma}_X(p^2)}{p^2 + \hat{\Sigma}_\gamma(p^2)}\right]^2 \hat{P}_Z(p^2) \,,$$
$$\hat{P}_X(p^2) \;=\; \left[\frac{-\hat{\Sigma}_X(p^2)}{p^2 + \hat{\Sigma}_\gamma(p^2)}\right] \hat{P}_Z(p^2) \,,$$

[1] Note that the real and imaginary parts of the complex vector-boson masses can be related by means of the optical theorem [8].

$$\hat{P}_Z(p^2) = \left[\frac{p^2-\mu_Z}{p^2-\mu_Z+\hat{Z}(p^2)-\hat{Z}(\mu_Z)}\right]\frac{1}{p^2-\mu_Z}\,,$$
$$\hat{P}_W(p^2) = \left[\frac{p^2-\mu_W}{p^2-\mu_W+\hat{\Sigma}_W(p^2)-\hat{\Sigma}_W(\mu_W)}\right]\frac{1}{p^2-\mu_W}\,. \tag{7}$$

Now we can renormalize the bare couplings by expressing them in terms of running couplings[2]:

$$\frac{e^2(p^2)}{\hat{e}^2} = \frac{p^2}{p^2+\hat{\Sigma}_\gamma(p^2)}\,, \tag{8}$$
$$\frac{g_w^2(p^2)}{\hat{g}_w^2} = \frac{p^2}{p^2+\hat{\overline{\Sigma}}_W(p^2)}\,, \tag{9}$$
$$\frac{s_w^2(p^2)}{\hat{s}_w^2} = \frac{p^2+\hat{\overline{\Sigma}}_W(p^2)}{p^2+\hat{\Sigma}_\gamma(p^2)}\,, \tag{10}$$

which fulfill, in analogy to the bare relation $\hat{g}_w^2 = \hat{e}^2/(2\hat{s}_w^2)$, the relation

$$g_w^2(p^2) = \frac{e^2(p^2)}{2s_w^2(p^2)}\,. \tag{11}$$

This allows us to rewrite $\hat{Z}(p^2)$ using Eq.(3):

$$\frac{p^2+\hat{Z}(p^2)}{p^2} = \frac{\hat{g}_w^2}{\hat{c}_w^2}\left[\frac{c_w^2(p^2)}{g_w^2(p^2)}+\frac{T_Z(p^2)}{p^2}\right]\,, \tag{12}$$

with $c_w^2(p^2) \equiv 1-s_w^2(p^2)$. Using Eq.(9) and Eq.(12), we can rewrite the mass-renormalization conditions given in Eqs.(4–5) as

$$\frac{\hat{\mu}_W}{\mu_W} = \hat{g}_w^2\left[\frac{1}{g_w^2(\mu_W)}+\frac{T_W(\mu_W)}{\mu_W}\right]\,, \tag{13}$$
$$\frac{\hat{\mu}_Z}{\mu_Z} = \frac{\hat{g}_w^2}{\hat{c}_w^2}\left[\frac{c_w^2(\mu_Z)}{g_w^2(\mu_Z)}+\frac{T_Z(\mu_Z)}{\mu_Z}\right]\,. \tag{14}$$

2.3 Renormalized propagators and fermion–gauge-boson vertex functions

Using the results of the previous subsection, the bare propagators Eq.(7) can be expressed in terms of running couplings in the following way:

$$\hat{P}_\gamma(p^2) = \frac{e^2(p^2)}{\hat{e}^2}\,\frac{1}{p^2} \quad + \quad \frac{\hat{s}_w^2}{\hat{c}_w^2}\left[\frac{s_w^2(p^2)}{\hat{s}_w^2}-1\right]^2\hat{P}_Z(p^2)\,,$$

[2]It is not necessary to fix the input parameters in order to carry out the renormalization. The running couplings can be adjusted to input parameters later on (see App. C).

$$\hat{P}_X(p^2) = \frac{\hat{s}_w}{\hat{c}_w}\left[\frac{s_w^2(p^2)}{\hat{s}_w^2} - 1\right]\hat{P}_Z(p^2)\,,$$
$$\hat{P}_Z(p^2) = \frac{g_w^2(p^2)}{\hat{g}_w^2}\,\frac{\hat{c}_w^2}{c_w^2(p^2)}\,\frac{\chi_Z(p^2)}{p^2}\,,$$
$$\hat{P}_W(p^2) = \frac{g_w^2(p^2)}{\hat{g}_w^2}\,\frac{\chi_W(p^2)}{p^2}\,, \tag{15}$$

where we define the propagator functions $\chi_{Z,W}(p^2)/p^2$ by

$$\chi_Z^{-1}(p^2) = 1 - \frac{g_w^2(p^2)}{p^2\,c_w^2(p^2)}\left[\frac{\mu_Z\,c_w^2(\mu_Z)}{g_w^2(\mu_Z)} - T_Z(p^2) + T_Z(\mu_Z)\right]\,, \tag{16}$$
$$\chi_W^{-1}(p^2) = 1 - \frac{g_w^2(p^2)}{p^2}\left[\frac{\mu_W}{g_w^2(\mu_W)} - T_W(p^2) + T_W(\mu_W)\right]\,. \tag{17}$$

The so-defined propagator functions are finite, as the ultraviolet (UV) divergences in T_W and T_Z are independent of p^2 and hence cancel (see App. A). The propagator functions are real[3] for space-like p, i.e., $p^2 < 0$. This is easily seen, because the running couplings are real for $p^2 < 0$ owing to their definition, and the terms in Eqs.(16–17) involving μ_Z or μ_W combine to a real quantity owing to Eqs.(13–14).

The above expressions for the resummed propagators lead to very simple expressions for the photon–Z system. We write the fermionic corrections to the photon or Z boson coupled to massless fermions as

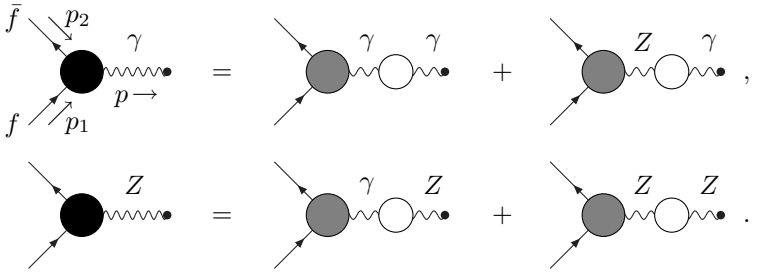

Here the open circles denote resummed propagators and the shaded circles vertex functions. The dot on the right-hand side of the diagrams indicates that the corresponding leg is not amputated, i.e., that the propagator is included. Since the fermion–gauge-boson vertex gets no fermionic corrections and thus enters only at Born level, the diagrams show the actual resummation of the propagators.

In order to investigate the implications of our renormalization prescription on these fermion–gauge-boson couplings, we introduce the unrenormalized fermion

[3]For time-like momenta ($p^2 > 0$) the original propagators contain a running width ($\propto p^2$). However, only a small and for large p^2 vanishing running-width component is retained in $p^2\chi_{Z,W}^{-1}(p^2)$. This is a consequence of having pulled out the running couplings from the original propagators, merely leaving behind $T_{Z,W}(p^2)$.

currents

$$\begin{aligned}
\hat{\Gamma}^{f}_{\gamma,\mu}(-p_2,p_1) &\equiv \hat{e}\;\bar{u}_f(-p_2)\,\gamma^\mu\,(-Q_f)\,u_f(p_1)\;,\\
\hat{\Gamma}^{f}_{z,\mu}(-p_2,p_1) &\equiv \hat{e}\;\bar{u}_f(-p_2)\,\gamma^\mu\,(\hat{v}_f-\hat{a}_f\gamma^5)\,u_f(p_1)\;,\\
\hat{\Gamma}^{f}_{w,\mu}(-p_2,p_1) &\equiv \hat{g}_w\;\bar{u}_f(-p_2)\,\gamma^\mu\,\omega_-u_{f'}(p_1)\;,
\end{aligned} \tag{18}$$

where $\omega_- = (1-\gamma_5)/2$, a minus sign in the argument of a u spinor indicates a v spinor, and f' represents the iso-spin partner of f. The electric charge fraction of the fermion f is denoted by Q_f, its iso-spin by I^3_f, and its bare couplings to the Z boson read

$$\hat{a}_f \equiv \frac{I^3_f}{2\hat{s}_w\hat{c}_w}\;, \qquad \hat{v}_f \equiv \hat{a}_f - Q_f\,\frac{\hat{s}_w}{\hat{c}_w}\;. \tag{19}$$

The renormalized fermion currents are analogously given by

$$\begin{aligned}
\Gamma^{f}_{\gamma,\mu}(-p_2,p_1) &\equiv e(p^2)\;\bar{u}_f(-p_2)\,\gamma^\mu\,(-Q_f)\,u_f(p_1)\;,\\
\Gamma^{f}_{z,\mu}(-p_2,p_1) &\equiv e(p^2)\;\bar{u}_f(-p_2)\,\gamma^\mu\,[v_f(p^2)-a_f(p^2)\gamma^5]\,u_f(p_1)\;,\\
\Gamma^{f}_{w,\mu}(-p_2,p_1) &\equiv g_w(p^2)\;\bar{u}_f(-p_2)\,\gamma^\mu\,\omega_-u_{f'}(p_1)\;,
\end{aligned} \tag{20}$$

where $p = p_1 + p_2$, and the running couplings $v_f(p^2)$ and $a_f(p^2)$ are defined as in Eq.(19) with $\hat{s}_w$ and $\hat{c}_w$ replaced by $s_w(p^2)$ and $c_w(p^2)$, respectively.

Now we can rewrite the fermion–Z-boson coupling including the Z and mixing propagators:

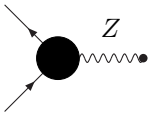

$$\begin{aligned}
\frac{\hat{e}}{\hat{s}_w\hat{c}_w} &= \left[\hat{\Gamma}^{f,\mu}_{\gamma}(-p_2,p_1)\;\hat{P}_x(p^2)+\hat{\Gamma}^{f,\mu}_{z}(-p_2,p_1)\;\hat{P}_z(p^2)\right]\frac{\hat{e}}{\hat{s}_w\hat{c}_w}\\
&= \Gamma^{f,\mu}_{z}(-p_2,p_1)\;\frac{\chi_z(p^2)}{p^2}\;\frac{e(p^2)}{c_w(p^2)s_w(p^2)}\\
&\equiv
\end{aligned}$$

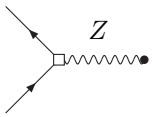

$$\frac{e(p^2)}{c_w(p^2)s_w(p^2)}\;, \tag{21}$$

where we denote the renormalized effective Born couplings of the fermions to the vector bosons by a box. The gauge bosons attached to such a box are defined to have their propagators replaced by the corresponding renormalized propagator functions [Eqs.(16–17)]. The effect of the renormalization is apparently to change all bare couplings to renormalized (running) ones and the Z propagator to $\chi_z(p^2)/p^2$.

Similarly the fermion–photon interaction can be written as

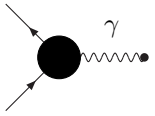

$$\hat{e} \;=\; \left[\hat{\Gamma}^{f,\mu}_{\gamma}(-p_2,p_1)\;\hat{P}_\gamma(p^2)+\hat{\Gamma}^{f,\mu}_{z}(-p_2,p_1)\;\hat{P}_x(p^2)\right]\hat{e}$$

$$
\begin{aligned}
&= \Gamma_{\gamma}^{f,\mu}(-p_2,p_1)\,\frac{1}{p^2}\,e(p^2) \\
&\quad + \Gamma_{Z}^{f,\mu}(-p_2,p_1)\,\frac{\chi_Z(p^2)}{p^2}\,\frac{e(p^2)}{c_w(p^2)s_w(p^2)}\,\left(s_w^2(p^2)-\hat{s}_w^2\right)
\end{aligned}
$$

$\equiv$ 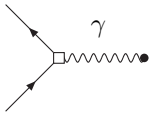 $e(p^2)$

$+$ 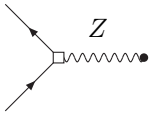 $\dfrac{e(p^2)}{c_w(p^2)s_w(p^2)}\,\left(s_w^2(p^2)-\hat{s}_w^2\right)\,.$

(22)

In this case some bare couplings are still left, but in specific processes involving massless fermionic final states (e.g. four-fermion processes at LEP1, six-fermion processes at LEP2) the fermion–photon interactions usually appear in the following two combinations:

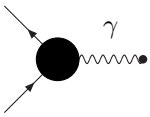 $\hat{e}\;-$ 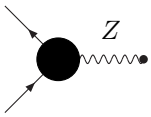 $\hat{e}\,\dfrac{\hat{c}_w}{\hat{s}_w}\;=$

$=$ 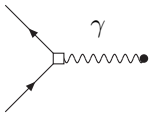 $e(p^2)\;-$ 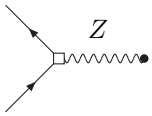 $e(p^2)\,\dfrac{c_w(p^2)}{s_w(p^2)}$ (23)

and

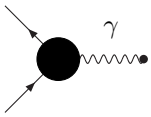 $\hat{e}\;+$ 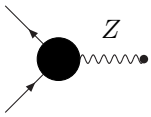 $\hat{e}\,\dfrac{\hat{s}_w}{\hat{c}_w}\;=$

$=$ 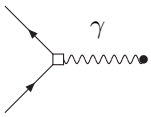 $e(p^2)\;+$ 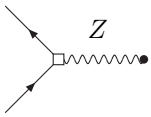 $e(p^2)\,\dfrac{s_w(p^2)}{c_w(p^2)}\,.$ (24)

In these combinations all bare quantities have combined into renormalized (running) couplings.

The fermion–W-boson interaction yields in an analogous way

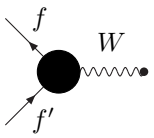

$$\hat{g}_w = \hat{\Gamma}^{f,\mu}_{W}(-p_2,p_1)\,\hat{P}_W(p^2)\,\hat{g}_w$$

$$= \Gamma^{f,\mu}_{W}(-p_2,p_1)\,\frac{\chi_W(p^2)}{p^2}\,g_w(p^2)$$

$$\equiv$$

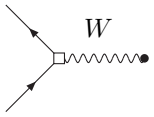

$$g_w(p^2)\,. \qquad (25)$$

The above effective interactions are essential ingredients for constructing renormalized, resummed amplitudes for LEP1 and LEP2 processes.

2.4 The process $e^+e^- \to f\bar{f}$

As an example of the renormalization procedure we discuss the four-fermion process $e^+(p_2)e^-(p_1) \to f(q_1)\bar{f}(q_2)$ with massless external fermions. If the fermion f is not in the same doublet as the electron, the bare amplitude is given by the sum of the following sub-amplitudes ($p = p_1 + p_2$):

$$\begin{aligned}
\mathcal{M}_1^{ee;\,ff}(-p_2,p_1;\,q_1,-q_2) &= \mathcal{M}_{\gamma\gamma} + \mathcal{M}_{Z\gamma} + \mathcal{M}_{ZZ} + \mathcal{M}_{\gamma Z}\,, \\
\mathcal{M}_{\gamma\gamma} &= \hat{\Gamma}^{e}_{\gamma,\mu}(-p_2,p_1)\,\hat{P}_\gamma(p^2)\,\hat{\Gamma}^{f,\mu}_{\gamma}(q_1,-q_2)\,, \\
\mathcal{M}_{Z\gamma} &= \hat{\Gamma}^{e}_{Z,\mu}(-p_2,p_1)\,\hat{P}_X(p^2)\,\hat{\Gamma}^{f,\mu}_{\gamma}(q_1,-q_2)\,, \\
\mathcal{M}_{ZZ} &= \hat{\Gamma}^{e}_{Z,\mu}(-p_2,p_1)\,\hat{P}_Z(p^2)\,\hat{\Gamma}^{f,\mu}_{Z}(q_1,-q_2)\,, \\
\mathcal{M}_{\gamma Z} &= \hat{\Gamma}^{e}_{\gamma,\mu}(-p_2,p_1)\,\hat{P}_X(p^2)\,\hat{\Gamma}^{f,\mu}_{Z}(q_1,-q_2)\,. \qquad (26)
\end{aligned}$$

Exploiting the results of the last subsection, these sub-amplitudes combine as follows

$\mathcal{M}_1^{ee;\,ff}(-p_2,p_1;\,q_1,-q_2) =$

$=$

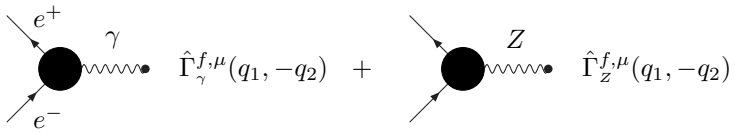

$$\hat{\Gamma}^{f,\mu}_{\gamma}(q_1,-q_2) \quad + \quad \hat{\Gamma}^{f,\mu}_{Z}(q_1,-q_2)$$

$=$

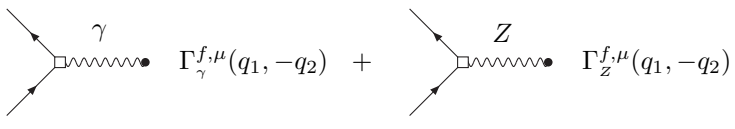

$$\Gamma^{f,\mu}_{\gamma}(q_1,-q_2) \quad + \quad \Gamma^{f,\mu}_{Z}(q_1,-q_2)$$

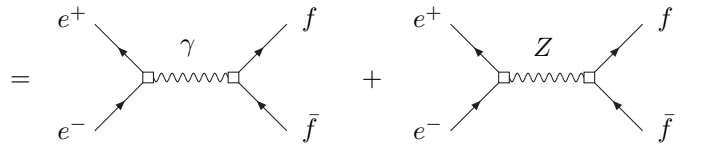

(27)

So, we arrive at a finite, effective Born amplitude in terms of running couplings and propagator functions

$$\mathcal{M}_1^{ee;\,ff}(-p_2,p_1;\,q_1,-q_2) = \Gamma_{\gamma}^{e,\mu}(-p_2,p_1)\,\frac{1}{p^2}\,\Gamma^{f}_{\gamma,\mu}(q_1,-q_2) + \Gamma_{Z}^{e,\mu}(-p_2,p_1)\,\frac{\chi_Z(p^2)}{p^2}\,\Gamma^{f}_{Z,\mu}(q_1,-q_2)\,. \quad (28)$$

The amplitude for Bhabha scattering, $e^+e^- \to e^+e^-$, is given in terms of the above amplitudes as $\mathcal{M}_1^{ee;\,ee}(-p_2,p_1;\,q_1,-q_2) - \mathcal{M}_1^{ee;\,ee}(-p_2,-q_2;\,q_1,p_1)$. In the second term the interchange of $-q_2$ and p_1 also applies to the definition of the gauge-boson momentum p.

Processes that can also proceed via the charged current require an additional basic amplitude, involving the exchange of a W boson ($q = p_2 - q_2$):

$$\mathcal{M}_2^{ff';\,\nu_e e}(-p_2,-q_2;\,q_1,p_1) = \Gamma_{W}^{f,\mu}(-p_2,-q_2)\,\frac{\chi_W(q^2)}{q^2}\,\Gamma^{\nu_e}_{W,\mu}(q_1,p_1)\,. \quad (29)$$

Therewith the full renormalized amplitude for $e^+e^- \to \nu_e\bar{\nu}_e$ is given by the combination $\mathcal{M}_1^{ee;\,\nu_e\nu_e}(-p_2,p_1;\,q_1,-q_2) - \mathcal{M}_2^{e\nu_e;\,\nu_e e}(-p_2,-q_2;\,q_1,p_1)$. Finally the renormalized amplitude for the muon decay $\mu(p) \to \nu_\mu(q_1)e(q_2)\bar{\nu}_e(q_3)$ reads $\mathcal{M}_2^{\nu_\mu\mu;\,e\nu_e}(q_1,p;\,q_2,-q_3)$.

3 The triple gauge-boson vertex

Besides the measurement of the W-boson mass, the main object of study in LEP2 processes will be the triple gauge-boson vertex. In this section we discuss the fermionic one-loop corrections to this vertex. First the full gauge-boson vertex functions, including fermionic corrections, are split into bare couplings and finite coefficients. Then the Ward identities for the triple gauge-boson vertices are given, from which the Ward identities for the finite coefficients and subsequently those for the full renormalized gauge-boson vertex functions are inferred. Using the results of Section 2 for the renormalized fermion–gauge-boson interactions, basic matrix elements for LEP2 processes are constructed. Finally, the gauge invariance of the renormalized LEP2 amplitudes is verified through these basic matrix elements.

3.1 The unrenormalized triple gauge-boson vertex

Like the gauge-boson self-energies, the gauge-boson vertex functions can be split into a photonic piece, G^γ, and an iso-spin part, G^I, that vanishes with vanishing

fermion masses and that is dominated by the top-quark contribution:

$$\hat{V}^{\{\gamma,Z\}W^+W^-}_{\mu\kappa\lambda}(q,p_+,p_-) = \left\{1, -\frac{\hat{c}_w}{\hat{s}_w}\right\} \hat{e}\hat{g}_w^2\, G^{\gamma}_{\mu\kappa\lambda}(q,p_+,p_-) + \{0,1\}\, \frac{\hat{e}\hat{g}_w^2}{\hat{s}_w\hat{c}_w}\, G^{I}_{\mu\kappa\lambda}(q,p_+,p_-)\,. \tag{30}$$

Here and in the following all particles and momenta are defined to be incoming. The first term in the curly brackets refers to the photon, the second term to the Z boson. In LEP2 processes the vertex functions $\hat{V}^{\gamma WW}$ and $\hat{V}^{ZWW}$ are contracted with external massless fermionic currents and appear in two distinct combinations. The combinations of couplings appearing in Eq.(30) are of the form described in Eq.(23) and Eq.(21). Hence, if the coefficients G^{γ} and G^{I} are finite, also the triple gauge-boson vertex functions yield finite contributions to the LEP2 amplitudes, with all bare couplings replaced by renormalized (running) ones.

The one-loop contributions to the coefficients G^{γ} and G^{I} are given in App. B. The pure one-loop coefficient $G^{I,(1)} = G^{I}$ is finite. The coefficient G^{γ} can be decomposed into tree-level and one-loop contributions according to

$$\begin{aligned} G^{\gamma}_{\mu\kappa\lambda}(q,p_+,p_-) &= \frac{1}{\hat{g}_w^2}\,\Gamma_{\mu\kappa\lambda}(q,p_+,p_-) + G^{\gamma,\,(1)}_{\mu\kappa\lambda}(q,p_+,p_-) \\ &= \left[\frac{1}{g_w^2(q^2)} - \frac{\hat{\overline{\Sigma}}_W(q^2)}{q^2\hat{g}_w^2}\right]\,\Gamma_{\mu\kappa\lambda}(q,p_+,p_-) + G^{\gamma,\,(1)}_{\mu\kappa\lambda}(q,p_+,p_-)\,, \end{aligned} \tag{31}$$

containing the lowest-order vertex tensor

$$\Gamma_{\mu\kappa\lambda}(q,p_+,p_-) = (q-p_+)_\lambda\, g_{\mu\kappa} + (p_+-p_-)_\mu\, g_{\kappa\lambda} + (p_- - q)_\kappa\, g_{\lambda\mu}\,. \tag{32}$$

The tree-level part of G^{γ} gives rise to an UV-divergent term, indicated by $-\hat{\overline{\Sigma}}_W(q^2)/(q^2\hat{g}_w^2)$. This term cancels the UV divergences contained in $G^{\gamma,\,(1)}$ (see App. B). So both G^{γ} and G^{I} are finite.

3.2 Ward identities for the triple gauge-boson vertex

At the level of Green functions the underlying gauge symmetry manifests itself in Ward identities, which in particular rule the gauge cancellations. Since we only deal with fermionic one-loop corrections we need those Ward identities that hold for these corrections and the tree-level expressions. They can be obtained from the general Ward identities of gauge theories [10] by omitting all other contributions. Alternatively, one can directly take over the background-field Ward identities [6] as the fermion-loop contributions are identical in the conventional approach and the background-field formalism.

For the bare vertex functions $\hat{V}^{\gamma W^+W^-}$, $\hat{V}^{ZW^+W^-}$, $\hat{V}^{\gamma W^+\phi^-}$, $\hat{V}^{ZW^+\phi^-}$, and $\hat{V}^{\chi W^+W^-}$ these Ward identities are given by:

$$
\begin{aligned}
& q^\mu\, \hat{V}^{\{\gamma,Z\}W^+W^-}_{\mu\kappa\lambda}(q,p_+,p_-) - i\,\sqrt{\hat{\mu}_Z}\,\{0,1\}\,\hat{V}^{\chi W^+W^-}_{\kappa\lambda}(q,p_+,p_-) = \\
& \quad \hat{e}\left\{1,-\frac{\hat{c}_w}{\hat{s}_w}\right\}\Bigg[T_{\kappa\lambda}(p_-)\,\left(p_-^2+\hat{\Sigma}_W(p_-^2)\right) + L_{\kappa\lambda}(p_-)\,\hat{\Sigma}_{W,L}(p_-^2) \\
& \qquad\qquad - T_{\kappa\lambda}(p_+)\,\left(p_+^2+\hat{\Sigma}_W(p_+^2)\right) - L_{\kappa\lambda}(p_+)\,\hat{\Sigma}_{W,L}(p_+^2)\Bigg]\,, \qquad (33)
\end{aligned}
$$

$$
\begin{aligned}
& -p_-^\lambda\, \hat{V}^{\{\gamma,Z\}W^+W^-}_{\mu\kappa\lambda}(q,p_+,p_-) - \sqrt{\hat{\mu}_W}\,\hat{V}^{\{\gamma,Z\}W^+\phi^-}_{\mu\kappa}(q,p_+,p_-) = \\
& \quad \hat{e}\left\{1,-\frac{\hat{c}_w}{\hat{s}_w}\right\}\Bigg[T_{\mu\kappa}(q)\,\left(q^2+\hat{\Sigma}_{\{\gamma,Z\}}(q^2) - \left\{\frac{\hat{c}_w}{\hat{s}_w},\frac{\hat{s}_w}{\hat{c}_w}\right\}\hat{\Sigma}_X(q^2)\right) \\
& \qquad\qquad + \{0,1\}\,\left(L_{\mu\kappa}(q)\,\hat{\Sigma}_{Z,L}(q^2) - g_{\mu\kappa}\,\hat{\mu}_Z\right) \\
& \qquad\qquad - T_{\mu\kappa}(p_+)\,\left(p_+^2+\hat{\Sigma}_W(p_+^2)\right) - L_{\mu\kappa}(p_+)\,\hat{\Sigma}_{W,L}(p_+^2) + g_{\mu\kappa}\,\hat{\mu}_W\Bigg]\,, \qquad (34)
\end{aligned}
$$

and an analogous Ward identity for the external W^+ leg. While the longitudinal parts of the photon self-energy and the photon–Z mixing energy vanish, those of the W and Z self-energies, $\hat{\Sigma}_{W,L}$ and $\hat{\Sigma}_{Z,L}$, appear explicitly in the Ward identities. Note that we have introduced the following transverse and longitudinal tensors:

$$
T_{\mu\nu}(p) \equiv g_{\mu\nu} - p_\mu p_\nu/p^2, \qquad L_{\mu\nu}(p) \equiv p_\mu p_\nu/p^2\,. \qquad (35)
$$

The vertex functions involving the Higgs ghosts, χ and $\phi^\pm$, can be split up in the same way as the gauge-boson vertex functions:

$$
\begin{aligned}
\sqrt{\hat{\mu}_Z}\,\hat{V}^{\chi W^+W^-}_{\kappa\lambda}(q,p_+,p_-) &= \frac{\hat{e}\hat{g}_w^2}{\hat{s}_w\hat{c}_w}\,X_{\kappa\lambda}(q,p_+,p_-)\,, \\
\sqrt{\hat{\mu}_W}\,\hat{V}^{\{\gamma,Z\}W^+\phi^-}_{\mu\kappa}(q,p_+,p_-) &= \left\{1,-\frac{\hat{c}_w}{\hat{s}_w}\right\}\,\hat{e}\hat{g}_w^2\,F^\gamma_{\mu\kappa}(q,p_+,p_-) \\
&\quad + \{0,1\}\,\frac{\hat{e}\hat{g}_w^2}{\hat{s}_w\hat{c}_w}\,F^I_{\mu\kappa}(q,p_+,p_-)\,. \qquad (36)
\end{aligned}
$$

As the fermion–Higgs-ghost couplings are proportional to the fermion masses, these vertex functions involve apart from the tree-level contributions,

$$
\begin{aligned}
X^{(0)}_{\kappa\lambda}(q,p_+,p_-) &= 0\,, \\
F^{\gamma,(0)}_{\mu\kappa}(q,p_+,p_-) &= F^{I,(0)}_{\mu\kappa}(q,p_+,p_-) = -\frac{\hat{\mu}_W}{\hat{g}_w^2}\,g_{\mu\kappa}\,, \qquad (37)
\end{aligned}
$$

predominantly top-quark contributions. Note that the ratio $\hat{\mu}_W/\hat{g}_w^2$ is not finite, its UV divergence equals the one contained in T_W [see Eq.(13)] and is canceled by the top-mass dependent one-loop corrections $F^{\gamma,(1)}$ and $F^{I,(1)}$.

Using Eq.(3), the definitions of the running couplings Eqs.(8–10), and the propagator functions Eqs.(16–17), we can rewrite the Ward identities in terms of the coefficients:

$$
\begin{aligned}
q^\mu\, G^\gamma_{\mu\kappa\lambda}(q,p_+,p_-) \;=\; & \frac{T_{\kappa\lambda}(p_-)}{g_w^2(p_-^2)}\,\frac{p_-^2}{\chi_W(p_-^2)} + L_{\kappa\lambda}(p_-)\,\frac{\hat\Sigma_{W,L}(p_-^2)-\hat\mu_W}{\hat g_w^2} \\
& - \frac{T_{\kappa\lambda}(p_+)}{g_w^2(p_+^2)}\,\frac{p_+^2}{\chi_W(p_+^2)} - L_{\kappa\lambda}(p_+)\,\frac{\hat\Sigma_{W,L}(p_+^2)-\hat\mu_W}{\hat g_w^2}\;, \\
q^\mu\, G^I_{\mu\kappa\lambda}(q,p_+,p_-) \;=\; & i\,X_{\kappa\lambda}(q,p_+,p_-)\;, \\
-p_-^\lambda\, G^\gamma_{\mu\kappa\lambda}(q,p_+,p_-) \;=\; & F^\gamma_{\mu\kappa}(q,p_+,p_-) + \frac{T_{\mu\kappa}(q)}{g_w^2(q^2)}\,q^2 \\
& - \frac{T_{\mu\kappa}(p_+)}{g_w^2(p_+^2)}\,\frac{p_+^2}{\chi_W(p_+^2)} - L_{\mu\kappa}(p_+)\,\frac{\hat\Sigma_{W,L}(p_+^2)-\hat\mu_W}{\hat g_w^2}\;, \\
-p_-^\lambda\, G^I_{\mu\kappa\lambda}(q,p_+,p_-) \;=\; & F^I_{\mu\kappa}(q,p_+,p_-) - \frac{T_{\mu\kappa}(q)}{g_w^2(q^2)}\,c_w^2(q^2)\,\left[\frac{q^2}{\chi_Z(q^2)} - q^2\right] \\
& - L_{\mu\kappa}(q)\,\hat c_w^2\,\frac{\hat\Sigma_{Z,L}(q^2)-\hat\mu_Z}{\hat g_w^2}\;.
\end{aligned}
\tag{38}
$$

All terms in these Ward identities are finite, including the factors that multiply the longitudinal tensors. This is caused by the fact that the quantities $\hat\mu_W/\hat g_w^2$, $\hat\Sigma_{W,L}/\hat g_w^2$, and $\hat c_w^2\,\hat\Sigma_{Z,L}/\hat g_w^2$ contain the same UV divergence.

Defining the renormalized vertex functions as

$$
\begin{aligned}
V^{\{\gamma,Z\}W^+W^-}_{\mu\kappa\lambda}(q,p_+,p_-) \equiv & \left\{1, -\frac{c_w(q^2)}{s_w(q^2)}\right\}\, e(q^2) g_w(p_+^2) g_w(p_-^2)\, G^\gamma_{\mu\kappa\lambda}(q,p_+,p_-) \\
& + \{0,1\}\,\frac{e(q^2) g_w(p_+^2) g_w(p_-^2)}{s_w(q^2) c_w(q^2)}\, G^I_{\mu\kappa\lambda}(q,p_+,p_-)\;, \\
\sqrt{\mu_z}\, V^{\chi W^+W^-}_{\kappa\lambda}(q,p_+,p_-) \equiv & \frac{e(q^2) g_w(p_+^2) g_w(p_-^2)}{s_w(q^2) c_w(q^2)}\, X_{\kappa\lambda}(q,p_+,p_-)\;, \\
\sqrt{\mu_W} V^{\{\gamma,Z\}W^+\phi^-}_{\mu\kappa}(q,p_+,p_-) \equiv & \left\{1, -\frac{c_w(q^2)}{s_w(q^2)}\right\}\, e(q^2) g_w(p_+^2) g_w(p_-^2) F^\gamma_{\mu\kappa}(q,p_+,p_-) \\
& + \{0,1\}\,\frac{e(q^2) g_w(p_+^2) g_w(p_-^2)}{s_w(q^2) c_w(q^2)}\, F^I_{\mu\kappa}(q,p_+,p_-)\;,
\end{aligned}
\tag{39}
$$

we can write down the Ward identities after renormalization. As we are going to investigate LEP2 processes, which involve only massless fermionic currents, all uncontracted external legs couple to conserved currents. As such all terms in the Ward identities involving explicit momentum vectors drop out and only the terms proportional to the metric tensors survive. The final form of the Ward identities, to be used in the following, is then given by

$$
q^\mu\, V^{\{\gamma,Z\}W^+W^-}_{\mu\kappa\lambda}(q,p_+,p_-) - i\,\sqrt{\mu_z}\,\{0,1\}\, V^{\chi W^+W^-}_{\kappa\lambda}(q,p_+,p_-) =
$$

$$e(q^2)\left\{1,-\frac{c_w(q^2)}{s_w(q^2)}\right\} g_w(p_+^2)g_w(p_-^2)\left[\frac{g_{\kappa\lambda}\,p_-^2}{g_w^2(p_-^2)\,\chi_W(p_-^2)}-\frac{g_{\kappa\lambda}\,p_+^2}{g_w^2(p_+^2)\,\chi_W(p_+^2)}\right]$$
$$+\,\text{terms vanishing for conserved external currents}\,, \tag{40}$$

$$-p_-^\lambda\, V_{\mu\kappa\lambda}^{\{\gamma,Z\}W^+W^-}(q,p_+,p_-)-\sqrt{\mu_W}\,V_{\mu\kappa}^{\{\gamma,Z\}W^+\phi^-}(q,p_+,p_-)=$$
$$e(q^2)\left\{1,-\frac{c_w(q^2)}{s_w(q^2)}\right\} g_w(p_+^2)g_w(p_-^2)\left[\frac{g_{\mu\kappa}}{g_w^2(q^2)}\left\{q^2,\frac{q^2}{\chi_Z(q^2)}\right\}-\frac{g_{\mu\kappa}\,p_+^2}{g_w^2(p_+^2)\,\chi_W(p_+^2)}\right]$$
$$+\,\text{terms vanishing for conserved external currents}\,. \tag{41}$$

These Ward identities are linear in the vertex functions and the inverse propagator functions.

3.3 Basic matrix elements for LEP2 processes

Combining the above results with the renormalized fermion–gauge-boson vertices given in Section 2, we are now in the position to introduce basic matrix elements for LEP2 processes, i.e., the six-fermion processes $e^-(p_1)e^+(p_2) \to f_1(q_1)f_2(q_2)\bar{f}_3(q_3)\bar{f}_4(q_4)$. Here all external fermions are taken to be massless. For the construction of the basic matrix elements it suffices to consider the situation that e, f_1, and f_2 are in different doublets. All other situations can be covered by interchanging particles in the basic matrix elements that are given below.

We first consider the basic matrix elements for W-pair-mediated LEP2 processes, i.e., $f_3 = f_1'$ and $f_4 = f_2'$. In order to identify the charge flow we assume the fermion f_1 to have negative charge. Using a box to indicate the renormalized triple gauge-boson vertex functions, the corresponding three basic matrix elements are given by (p_i incoming, q_i outgoing, $q = p_1 + p_2$, $p_+ = -q_1 - q_3$, $p_- = -q_2 - q_4$)

$$\mathcal{M}_1^{ee;\,f_1f_1';\,f_2f_2'}(-p_2,p_1;\,q_1,-q_3;\,q_2,-q_4) \;=$$

$=$

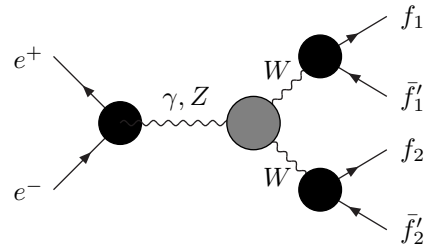

$$= \quad$$
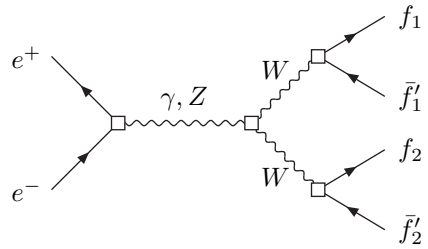

$$= \sum_{B=\gamma,Z} G_B^{e,\,\mu}(-p_2,p_1)\, V_{\mu\kappa\lambda}^{BW^+W^-}(q,p_+,p_-)\, G_W^{f_1,\,\kappa}(q_1,-q_3)\, G_W^{f_2,\,\lambda}(q_2,-q_4)\ ,$$

$\mathcal{M}_2^{ee;\,f_1f'_1;\,f_2f'_2}(-p_2,p_1;\,q_1,-q_3;\,q_2,-q_4) \;=$

$$= \quad$$
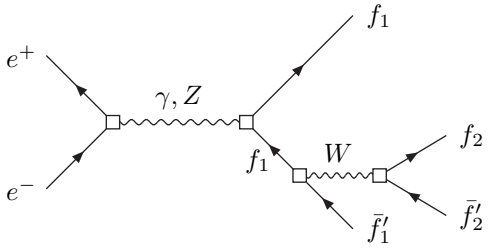

$$+ \quad$$
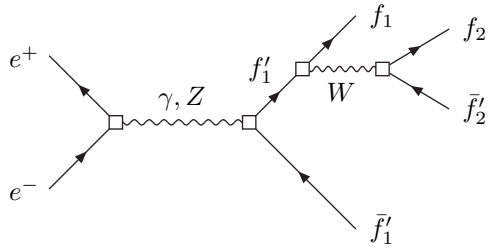

$$= -G_W^{f_2,\,\lambda}(q_2,-q_4)\, G_B^{e,\,\mu}(-p_2,p_1) \sum_{B=\gamma,Z} \Big[\Gamma_{BW,\,\mu\lambda}^{f_1f'_1}(q_1,q_1-q,-q_3) + \Gamma_{WB,\,\lambda\mu}^{f_1f'_1}(q_1,q_1-p_-,-q_3)\Big]\ ,$$

$\mathcal{M}_3^{ee;\,f_1f'_1;\,f_2f'_2}(-p_2,p_1;\,q_1,-q_3;\,q_2,-q_4) \;=$

$=$

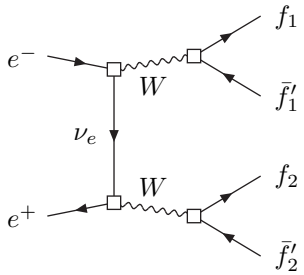

$$= -\Gamma^{ee}_{WW,\,\lambda\kappa}(-p_2, -p_2 - p_-, p_1)\, G_W^{f_1,\,\kappa}(q_1, -q_3)\, G_W^{f_2,\,\lambda}(q_2, -q_4)\,. \tag{42}$$

Here we introduced a couple of shorthand notations in order to keep the expressions as compact as possible ($B = \gamma, Z$):

$$\begin{aligned}
G_B^{f,\,\mu}(r,k) &= \Gamma_B^{f,\,\mu}(r,k)\,\frac{\chi_B(K^2)}{K^2}\,,\\
G_W^{f,\,\mu}(r,k) &= \Gamma_W^{f,\,\mu}(r,k)\,\frac{\chi_W(K^2)}{K^2}\,,\\
\Gamma^{ff,\,\mu\nu}_{WW}(p,r,k) &= g_w(P^2)\,g_w(K^2)\,\bar{u}_f(p)\,\gamma^\mu\,\frac{\not{r}}{r^2}\,\gamma^\nu\,\omega_-\,u_f(k)\,,\\
\Gamma^{ff',\,\mu\nu}_{BW}(p,r,k) &= e(P^2)\,[v_f^B(P^2) + a_f^B(P^2)]\,g_w(K^2)\,\bar{u}_f(p)\,\gamma^\mu\,\frac{\not{r}}{r^2}\,\gamma^\nu\,\omega_-\,u_{f'}(k)\,,\\
\Gamma^{ff',\,\mu\nu}_{WB}(p,r,k) &= g_w(P^2)e(K^2)\,[v_{f'}^B(K^2) + a_{f'}^B(K^2)]\,\bar{u}_f(p)\,\gamma^\mu\,\frac{\not{r}}{r^2}\,\gamma^\nu\,\omega_-\,u_{f'}(k)\,,\\
\Gamma^{ff,\,\mu\nu}_{B_1B_2}(p,r,k) &= e(P^2)e(K^2)\,\bar{u}_f(p)\,\gamma^\mu\,[v_f^{B_1}(P^2) - a_f^{B_1}(P^2)\gamma_5]\,\frac{\not{r}}{r^2}\\
&\qquad\times\,\gamma^\nu\,[v_f^{B_2}(K^2) - a_f^{B_2}(K^2)\gamma_5]\,u_f(k)\,,
\end{aligned} \tag{43}$$

with $\chi_\gamma(K^2) = 1$, $P = p - r$, $K = k - r$, and v_f^B and a_f^B denoting the vector and axial-vector couplings of the fermion f to the neutral gauge boson B ($v_f^Z = v_f$, $a_f^Z = a_f$, $v_f^\gamma = -Q_f$, $a_f^\gamma = 0$).

For the remaining, neutral-gauge-boson-mediated LEP2 processes, i.e., $f_3 = f_1$ and $f_4 = f_2$, two additional basic matrix elements are required. The first one originates from the triple gauge-boson vertices involving only neutral gauge bosons. These (C–odd and CP–even) vertices do not exist at lowest order and only receive contributions from ε-tensor terms, entering through the fermionic one-loop corrections. As all gauge bosons are neutral, no charge assignment is required. Writing $k_1 = p_1 + p_2$, $k_2 = -q_1 - q_3$, and $k_3 = -q_2 - q_4$, the basic matrix element reads

$$\mathcal{M}_4^{ee;\,f_1f_1;\,f_2f_2}(-p_2, p_1;\, q_1, -q_3;\, q_2, -q_4) \;=$$

$=$

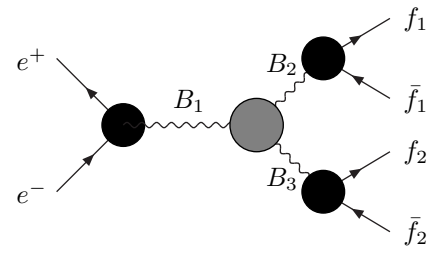

$=$

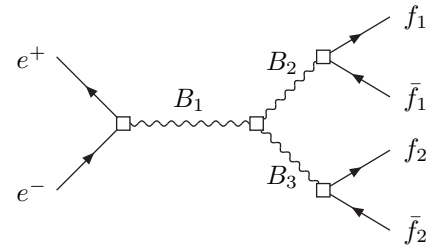

$$= \sum_{B_i=\gamma,Z} G^{e,\,\mu}_{B_1}(-p_2,p_1)\, V^{B_1B_2B_3}_{\mu\kappa\lambda}(k_1,k_2,k_3)\, G^{f_1,\,\kappa}_{B_2}(q_1,-q_3)\, G^{f_2,\,\lambda}_{B_3}(q_2,-q_4)\ . \tag{44}$$

The renormalized vertex function $V^{B_1B_2B_3}_{\mu\kappa\lambda}(k_1,k_2,k_3)$ is given by Eq.(71) in App. B.2 with $\hat{e}^3 \to e(k_1^2)\,e(k_2^2)\,e(k_3^2)$, $\hat{v}_f^{B_i} \to v_f^{B_i}(k_i^2)$, and $\hat{a}_f^{B_i} \to a_f^{B_i}(k_i^2)$. It obeys simple Ward identities of the form:

$$k_1^\mu\, V^{B_1B_2B_3}_{\mu\kappa\lambda}(k_1,k_2,k_3) = i\,\sqrt{\mu_Z}\,\delta_{B_1Z}\, V^{\chi B_2B_3}_{\kappa\lambda}(k_1,k_2,k_3) \qquad \text{for} \quad B_i=\gamma,Z\ . \tag{45}$$

The second basic matrix element for neutral-gauge-boson-mediated LEP2 processes is given by

$$\mathcal{M}_5^{ee;\,f_1f_1;\,f_2f_2}(-p_2,p_1;\,q_1,-q_3;\,q_2,-q_4) \;=$$

$=$

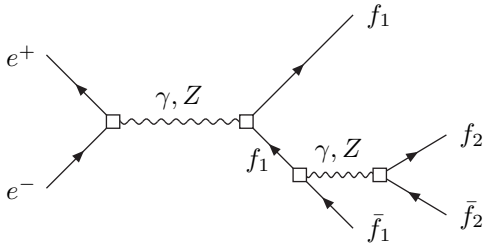

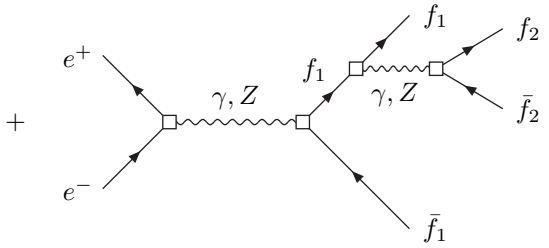

$$= -\sum_{B_1,B_2=\gamma,Z} G^{e,\mu}_{B_1}(-p_2,p_1)\, G^{f_2,\lambda}_{B_2}(q_2,-q_4)\, \Big[\Gamma^{f_1 f_1}_{B_1 B_2,\,\mu\lambda}(q_1,q_1-k_1,-q_3) + \Gamma^{f_1 f_1}_{B_2 B_1,\,\lambda\mu}(q_1,k_1-q_3,-q_3)\Big]\ . \tag{46}$$

From these basic matrix elements all amplitudes for massless six-fermion (LEP2) processes can be constructed (leaving out QCD diagrams).

3.4 Gauge invariance of renormalized LEP2 amplitudes

In the previous subsection the basic building blocks are provided for the construction of renormalized LEP2 amplitudes. As promised, we address now the issue of gauge invariance. After all, we have performed a resummation and subsequent renormalization of 1PI fermionic $\mathcal{O}(\alpha)$ corrections, which involves a different treatment of vertex corrections as compared to self-energy corrections. Such a procedure can be a possible source of gauge-invariance-breaking effects.

The U(1) gauge cancellations become numerically very important for electromagnetic interactions in the collinear limit, where the electromagnetic current $\Gamma^\mu_\gamma(r, r+k_\gamma)$ becomes proportional to the momentum of the internal photon k^μ_γ (with $k^2_\gamma \ll E^2_{CM}$). On the other hand, SU(2) gauge cancellations become relevant in the high-energy limit ($k^2_{W,Z} \ll E^2_{CM}$) if an external current coupled to a massive internal gauge boson becomes approximately proportional to the gauge-boson momentum, in other words the gauge boson is effectively longitudinal. From this it should be clear that in these regimes sensible theoretical predictions are only possible if the amplitudes with external currents replaced by the corresponding gauge-boson momenta fulfill appropriate Ward identities. When we talk about gauge invariance in this paper we always mean the validity of these Ward identities. The Ward identities explicitly read

$$k^\mu \mathcal{M}^\gamma_\mu = 0, \qquad k^\mu \mathcal{M}^Z_\mu = i\sqrt{\mu_z}\mathcal{M}^\chi, \qquad k^\mu \mathcal{M}^{W^\pm}_\mu = \pm\sqrt{\mu_w}\mathcal{M}^{\phi^\pm}\ , \tag{47}$$

where $\mathcal{M}^V_\mu$ ($V = \gamma, Z, W^\pm$) denote the amplitudes with the corresponding currents amputated. The first identity expresses transversality with respect to external photon momenta, the latter two imply the Goldstone-boson equivalence theorem.

The gauge invariance of the amplitudes that do not involve the triple gauge-boson vertex is evident. The same goes for the amplitudes of neutral-gauge-boson-mediated LEP2 processes. So, we restrict ourselves to verifying the gauge

invariance of the universal amplitudes for W-pair-mediated LEP2 processes, i.e., the processes $e^-e^+ \to f_1 f_2 \bar{f}_1' \bar{f}_2'$ with e, f_1, and f_2 assumed to be in different doublets. These universal amplitudes contribute to all W-pair-mediated processes. All other situations can be covered by adding extra universal amplitudes with interchanged particles. Hence, it suffices to check the gauge invariance of the universal amplitudes.

The universal amplitude, $\mathcal{M}_{WW}^{\rm univ}$, can be written in terms of the basic matrix elements presented in the previous subsection:

$$\begin{aligned}\mathcal{M}_{WW}^{\rm univ} = & \sum_{i=1}^{3} \mathcal{M}_i^{ee;\, f_1 f_1';\, f_2 f_2'}(-p_2, p_1;\, q_1, -q_3;\, q_2, -q_4) \\ & + \mathcal{M}_2^{ee;\, f_2 f_2';\, f_1 f_1'}(-p_2, p_1;\, q_2, -q_4;\, q_1, -q_3)\;, \end{aligned} \tag{48}$$

where as before the fermion f_1 has been assumed to have negative charge. First we verify the gauge invariance with respect to the internal (incoming) W^- boson by replacing $G_W^{f_2,\,\lambda}(q_2, -q_4)$ by p_-^λ. As the last term in Eq.(48) only involves an (incoming) W^+ boson and, hence, does not contain the $G_W^{f_2,\,\lambda}$ current, only the first set of three terms should be considered for this particular gauge-invariance check. Using Eq.(41) and the various definitions for the fermionic currents, one ends up with

$$\begin{aligned}\mathcal{M}_{WW}^{\rm univ} \longrightarrow\; & p_-^\lambda \sum_{B=\gamma,Z} G_B^{e,\,\mu}(-p_2, p_1)\, V_{\mu\kappa\lambda}^{BW^+W^-}(q, p_+, p_-)\, G_W^{f_1,\,\kappa}(q_1, -q_3) \\ & + G_W^{f_1,\,\kappa}(q_1, -q_3)\, g_w(p_+^2) g_w(p_-^2)\, \bar{u}_e(-p_2)\, \gamma_\kappa\, \omega_-\, u_e(p_1) \\ & - G_\gamma^{e,\,\mu}(-p_2, p_1)\, G_{W,\,\mu}^{f_1}(q_1, -q_3)\, e(q^2)\, \frac{p_+^2}{\chi_W(p_+^2)}\, \frac{g_w(p_-^2)}{g_w(p_+^2)} \\ & + G_Z^{e,\,\mu}(-p_2, p_1)\, G_{W,\,\mu}^{f_1}(q_1, -q_3)\, e(q^2)\, \frac{c_w(q^2)}{s_w(q^2)}\, \frac{p_+^2}{\chi_W(p_+^2)}\, \frac{g_w(p_-^2)}{g_w(p_+^2)} \\ = \; & -\sum_{B=\gamma,Z} G_B^{e,\,\mu}(-p_2, p_1)\, \sqrt{\mu_W}\, V_{\mu\kappa}^{BW^+\phi^-}(q, p_+, p_-)\, G_W^{f_1,\,\kappa}(q_1, -q_3)\;. \end{aligned} \tag{49}$$

The last expression exactly equals the contribution from the renormalized $\gamma W \phi$ and $ZW\phi$ vertices. The gauge invariance with respect to the internal (incoming) W^+ boson can be verified in an analogous way.

The gauge invariance with respect to the internal neutral gauge bosons is verified by replacing $G_B^{e,\,\mu}(-p_2, p_1)$ by q^μ for $B = \{\gamma, Z\}$. In this case the matrix element $\mathcal{M}_3$ should be left out, as it only involves W bosons. Using Eq.(40) we find

$$\begin{aligned}\mathcal{M}_{WW}^{\rm univ} \longrightarrow\; & q^\mu\, V_{\mu\kappa\lambda}^{\{\gamma,Z\}W^+W^-}(q, p_+, p_-)\, G_W^{f_1,\,\kappa}(q_1, -q_3)\, G_W^{f_2,\,\lambda}(q_2, -q_4) \\ & + G_W^{f_1,\,\kappa}(q_1, -q_3)\, G_{W,\,\kappa}^{f_2}(q_2, -q_4)\, e(q^2) \left\{1, -\frac{c_w(q^2)}{s_w(q^2)}\right\} \frac{p_+^2}{\chi_W(p_+^2)}\, \frac{g_w(p_-^2)}{g_w(p_+^2)} \\ & - G_W^{f_1,\,\kappa}(q_1, -q_3)\, G_{W,\,\kappa}^{f_2}(q_2, -q_4)\, e(q^2) \left\{1, -\frac{c_w(q^2)}{s_w(q^2)}\right\} \frac{p_-^2}{\chi_W(p_-^2)}\, \frac{g_w(p_+^2)}{g_w(p_-^2)} \end{aligned}$$

$$= i\sqrt{\mu_Z}\,\{0,1\}\,V^{\chi W^+W^-}_{\kappa\lambda}(q,p_+,p_-)\,G_W^{f_1,\kappa}(q_1,-q_3)\,G_W^{f_2,\lambda}(q_2,-q_4)\ . \quad (50)$$

For the Z boson the last expression exactly equals the contribution from the renormalized χWW vertex.

While for the amplitudes involving gauge bosons gauge cancellations are essential, the amplitudes involving the Higgs ghosts behave properly without cancellations.

4 Application of the fermion-loop scheme to typical LEP2 processes

The fermion-loop (FL) scheme allows to introduce finite-width effects into all tree-level (non-QCD) six-fermion matrix elements. In this section we illustrate the FL scheme using as examples the processes $e^-e^+ \to \mu^-\bar\nu_\mu u\bar d$ (also called CC10), $e^-e^+ \to s\bar c u\bar d$ (also called CC11), and $e^-e^+ \to e^-\bar\nu_e u\bar d$ (also called CC20) with massless external fermions. The relevant terminology has been introduced in Ref. [11] and the CC class of processes comprises production of up (anti-up) and anti-down (down) fermion pairs, $(U_i\bar D_i) + (D_j\bar U_j)$. These reactions include some of the most interesting processes for studies at LEP2 and beyond.

In all of them SU(2) gauge invariance is needed to guarantee the unitarity cancellations at high energies. A violation of SU(2) gauge invariance can be most easily seen in the simple CC10/11 processes, where the dominant contribution comes from the W-pair-production diagrams and the onset of a bad high-energy behavior is already appreciable around 1 TeV.

The CC20 process, on the other hand, is also sensitive to the breaking of U(1) gauge invariance in the collinear limit, while the SU(2)-gauge-invariance violation becomes sizeable only above 2 TeV.

4.1 Amplitudes

The amplitudes for the processes $e^-e^+ \to \mu^-\bar\nu_\mu u\bar d$ and $e^-e^+ \to s\bar c u\bar d$ are directly given by the universal amplitude Eq.(48) with $f_1 = \mu$, $f_2 = u$ and $f_1 = s$, $f_2 = u$, respectively.

The amplitude for the process $e^-(p_1)e^+(k_1) \to e^-(p_2)\bar\nu_e(k_2)u(p_u)\bar d(p_d)$ is given by the sum of the universal amplitude Eq.(48) and this universal amplitude with the initial-state positron and final-state electron interchanged,

$$\begin{aligned}
\mathcal{M}^{ee\to e\nu_e ud} = &\sum_{i=1}^{3}\mathcal{M}_i^{ee;\,e\nu_e;\,ud}(-k_1,p_1;\,p_2,-k_2;\,p_u,-p_d)\\
&+\mathcal{M}_2^{ee;\,ud;\,e\nu_e}(-k_1,p_1;\,p_u,-p_d;\,p_2,-k_2)\\
&-\sum_{i=1}^{3}\mathcal{M}_i^{ee;\,e\nu_e;\,ud}(p_2,p_1;\,-k_1,-k_2;\,p_u,-p_d)\\
&-\mathcal{M}_2^{ee;\,ud;\,e\nu_e}(p_2,p_1;\,p_u,-p_d;\,-k_1,-k_2)\ . \qquad (51)
\end{aligned}$$

As all these matrix elements are just linear combinations of universal matrix elements, the gauge invariance follows directly from the discussion in Section 3.4.

For the CC20 process $e^-e^+ \to e^-\bar{\nu}_e u\bar{d}$ U(1) gauge invariance becomes essential in the region of phase space where the angle between the incoming and outgoing electrons is small [1, 2, 12, 13]. In this region of phase space the superficial $1/q_\gamma^4$ divergence, originating from the square of the photon propagator with momentum q_γ, is softened to $1/q_\gamma^2$ by U(1) gauge invariance. In the presence of light fermion masses this gives rise to the familiar $\log(m_e^2/s)$ large logarithms. In order to guarantee the softening of the $1/q_\gamma^4$ divergence, which is necessary for a meaningful cross-section, U(1) gauge invariance is required.

From the numerical point of view the SU(2) gauge invariance is not of real relevance at LEP2 energies, but it becomes important for energies reached at the next generation of linear colliders. It is important for all processes that involve the W-pair-production diagrams. At high energies, the SU(2) gauge invariance guarantees the gauge cancellations and thus ensures that the matrix element respects unitarity.

4.2 Input parameters

First we fix the input parameters. We work in a LEP2-like scheme [4], which uses the input parameters[4] $G_F, \mathrm{Re}\{\alpha_\ell(m_Z^2)^{-1}\}, m_Z, m_W$:

$$\begin{aligned} G_F &= 1.16639 \times 10^{-5}\ \mathrm{GeV}^{-2}\ , \\ \mathrm{Re}\{\alpha_\ell(m_Z^2)^{-1}\} &= 128.89\ , \\ m_W &= 80.26\ \mathrm{GeV}\ , \\ m_Z &= 91.1884\ \mathrm{GeV}\ . \end{aligned} \tag{52}$$

The electromagnetic coupling at the Z mass $\alpha_\ell(m_Z^2)$ (see analysis of Ref. [14]) differs slightly from our $\alpha(m_Z^2) = e^2(m_Z^2)/4\pi$, as top-quark effects are not included in the former.[5] Furthermore, m_W and m_Z are defined in the usual (LEP1) way, in which the renormalized mass is fixed by the zero of the real part of the inverse propagator. The masses of the light fermions (except top) are neglected.

With these input parameters we compute all bare parameters for some arbitrary value of the infinity Δ, taking into account that some input parameters are given in a different renormalization scheme. The knowledge of the bare parameters allows us to compute all running (renormalized) couplings of Eqs.(8–9) and the renormalized complex pole positions μ_W and μ_Z. An explicit computational scheme to accomplish this is given in App. C, where the LEP2 scheme is described within our fermion-loop approach, i.e., without any bosonic and QCD corrections. Note that the mass of the top quark is not an independent quantity

[4] We have used the same masses as in the analysis of Ref. [11]. The most recent values for $m_{Z,W}$ are 91.1863(20) GeV and 80.356(125) GeV.

[5] These effects are well approximated by $\alpha(m_Z^2)^{-1} - \alpha_\ell(m_Z^2)^{-1} = 4m_Z^2/(45\pi m_t^2) \approx 0.0282942\,(m_Z^2/m_t^2)$.

$m_{_W}$	80.10	80.26	80.42
m_t	104.768	132.185	157.195
$\sqrt{\mathrm{Re}\,\mu_{_W}}$	80.074	80.234	80.393
$-\mathrm{Im}\,\mu_{_W}/\sqrt{\mathrm{Re}\,\mu_{_W}}$	2.0377	2.0509	2.0636
$\sqrt{\mathrm{Re}\,\mu_{_Z}}$	91.1552	91.1550	91.1548
$-\mathrm{Im}\,\mu_{_Z}/\sqrt{\mathrm{Re}\,\mu_{_Z}}$	2.4538	2.4610	2.4688
$\mathrm{Re}\,e(m^2_{_W})$	0.311967	0.311979	0.311986
$\mathrm{Im}\,e(m^2_{_W})$	−0.002685	−0.002685	−0.002685
$\mathrm{Re}\,g_w(m^2_{_W})$	0.459802	0.460576	0.461400
$\mathrm{Im}\,g_w(m^2_{_W})$	−0.006450	−0.006482	−0.006516

Table 1: Values of the *effective* top-quark mass, pole positions, and effective couplings at $m^2_{_W}$ for three different W masses. All masses and pole-position-related quantities are given in GeV.

in this approach. In Table 1 we give the *effective* top-quark mass, the renormalized complex pole positions, and the complex couplings at $m^2_{_W}$ for three input W-boson masses $m_{_W}$.

The top-quark mass cannot be seen as more than an effective value, which partly compensates for the missing bosonic and QCD corrections, and hence it cannot be compared with the direct measurement [15]. Indeed the m_t–$m_{_H}$ connection plays a fundamental role and when we perform a more complete m_t-determination by including all the available radiative corrections in the on-shell scheme [4], we find a quite remarkable agreement with the experimental data.

The real and imaginary parts of the W and Z poles are described well by the approximative formulae $\mathrm{Re}\,\mu \approx m^2 - \Gamma^2$ and $\mathrm{Im}\,\mu \approx -m\Gamma + \Gamma^3/m$, respectively (see App. D). Here Γ is the gauge-boson width including fermionic corrections, calculated in the LEP1 scheme. For the W boson this corrected width is about 0.8% larger than the lowest-order width in the G_F parameterization [$= 3G_F m^3_{_W}/(2\sqrt{2}\pi)$]. This is in agreement with the arctangent term in Eq.(9) of Ref. [8].

4.3 Schemes

In the following we present numerical results obtained with the FL scheme and compare these with the results obtained with other schemes. The following schemes are considered in our analysis:

Running width: The cross-section is computed using the tree-level amplitude. The massive gauge-boson propagators acquire a running width for $p^2 > 0$:

$1/(p^2 - m^2 + ip^2\Gamma/m) = 1/([1 + i\Gamma/m][p^2 - m^2/(1 + i\Gamma/m)])$. Thus, for $p^2 > 0$ this scheme is nothing more than a fixed-width scheme with modified pole and residue. This scheme violates U(1) and SU(2) gauge invariance.

Fixed width: The cross-section is computed using the tree-level amplitude. The massive gauge-boson propagators are given by $1/(p^2 - m^2 + im\Gamma)$. This gives an unphysical width for $p^2 < 0$, but retains U(1) gauge invariance in the CC20 process [1]. For the considered six-fermion processes the SU(2) gauge violation is suppressed by $m\Gamma/s$ (at the matrix-element level) at high energies and therefore the high-energy behavior is consistent with unitarity. This scheme will exhibit a bad high-energy behavior when applied to processes involving more intermediate gauge bosons, e.g. processes with six fermions in the final state.

Running width + U(1)-invariance-restoring γWW vertex factor: This scheme was proposed in Ref. [1] as a simple and sufficiently accurate approach for LEP2 generators. It involves naive running widths for the massive gauge bosons, supplemented by a simple multiplicative factor for the γWW vertex (as derived in the limit $q_\gamma^2 \to 0$). By construction, U(1) gauge invariance is retained, but the SU(2) Ward identities are violated, rendering this scheme not appropriate for the high-energy regime.

Minimal FL scheme: A simplified minimal approach to incorporate the finite width, while ensuring both U(1) and SU(2) gauge invariance, consists in taking into account only the imaginary parts of the fermionic corrections in the massless limit. The top-quark mass is kept only in step functions that switch off the (massless) top contributions below the top thresholds [13].

Imaginary-part FL scheme: Now the full imaginary part of the fermion-loop corrections is used, leaving out all ε-tensor terms. The fermion masses are neglected except for the top-quark mass. This is the version of the FL scheme that was originally used in the analysis[6] of Ref. [1]. Once the massive top contributions are included this scheme is in fact not much easier than the complete FL scheme.

Full FL scheme: We take all fermion-loop contributions into account, but neglect all fermion masses except for the top-quark mass. The implementation of the fermionic one-loop corrections is rather straightforward (see Section 3.3). The tree-level couplings are replaced by running couplings at the appropriate momenta and the massive gauge-boson propagators by the functions $\chi_{\{W,Z\}}(p^2)/p^2$. The vertex coefficients G^γ and G^I, entering through the Yang–Mills vertex, contain the lowest-order couplings as well as the one-loop fermionic vertex corrections given in App. B.

[6] For the sake of clarity, the actual discussion and numbers presented in Ref. [1] were restricted to a U(1)-invariant subset of four diagrams involving near-collinear space-like photons. Moreover, the top contributions were not required in the case considered there.

In all schemes apart from the full FL scheme no non-imaginary higher-order corrections are included. In those schemes the values of the couplings have been determined from G_F, m_Z and m_W, as given in Eq.(52), in order to account for the most important universal corrections, i.e.,

$$g_w^2 = 2\sqrt{2}G_F m_W^2 = 0.212514, \qquad \alpha = \frac{g_w^2}{2\pi}\left(1 - \frac{m_W^2}{m_Z^2}\right) = 1/131.2145. \quad (53)$$

In the non-FL schemes the W-boson width has been determined in Born approximation without any QCD correction, giving $\Gamma_W = 2.03595\,\mathrm{GeV}$. In the FL schemes the top-quark mass has been set to $m_t = 132$ GeV, in accordance with the discussion in Section 4.2.

4.4 Numerical results

The theoretical results of the previous sections have been put into practice in computer programs. All the numbers presented in this section have been generated with three independently written Fortran programs: ERATO [16], WTO [17] and WWF [18]. While the minimal FL scheme is only implemented in ERATO and the imaginary-part fermion-loop scheme only in WTO, the other schemes are implemented in all three generators.

A detailed and tuned comparison was well beyond the purpose of the present work so that our numerical analysis, although reliable, is still far from the high-precision level reached in Ref. [11]. Whenever referring to the same setup (kinematical cuts etc.) we have found numerical results with a satisfactory agreement, within the quoted integration errors.

In this respect it should be noted that owing to the unitarity cancellations at high energies several digits, e.g., 6 digits at 10 TeV, cancel between the contribution of the neutrino-exchange and the other contributions of the W-pair-production diagrams. As compared with the standard formulation of the processes $e^-e^+ \to 4f$, also the average amount of needed CPU time has increased considerably due to the complexity of the new calculation. This fact alone is a justification of the relatively lower technical precision of our results when compared to the results presented in Ref. [11]. During the present analysis we have been mainly concerned in showing the feasibility of the project and paid less attention to the phenomenological side, thus most of our numerical results will be given without initial-state QED radiation (ISR). If not stated otherwise the canonical LEP2 cuts [11] are applied and no ISR is included.

In the discussion of the numerical results we focus on the two regions of phase-space where we expect gauge-invariance issues to play a role: small space-like q_γ^2 (collinear electron) and large $s = E_{CM}^2$. Apart from the experimentally relevant cross-sections at LEP2 energies with the canonical LEP2 cuts applied [11], we also give results for $e^-e^+ \to e^-\bar{\nu}_e u\bar{d}$ with only a cut on the angle between the final-state electron and either beam. This we do because most of the experimental analysis is currently done without imposing an energy threshold on the outgoing electron [19]. For very small scattering angles, however, it is

mandatory to use a fully massive phase space (and possibly matrix element), since the electron mass becomes essential[7] in the limit of very small initial-final invariant mass $(p_2 - p_1)^2$. In this respect it should be mentioned that the CC20 process is also needed to study the background to Higgs-boson production. This involves the so-called single-W events, with the outgoing electron lost in the beam pipe. In this case both a gauge-invariance-preserving scheme and the finite electron mass are needed.

For large s the W boson becomes effectively massless and W-bremsstrahlung becomes increasingly important. The matching negative virtual term, involving the exchange of W bosons, is not accounted for in our program and therefore we are obliged to make a cut on the outgoing W, or the highly correlated outgoing electron angle. We did not look into this any further since we are mainly interested in the SU(2) gauge cancellations that occur in *W-pair* production.

In the schemes described in Section 4.3 and for the CC20 process $e^-e^+ \to e^-\bar{\nu}_e u\bar{d}$, we have computed all quantities compared in Ref. [11]; the relevant ones are the first few moments of the angle of the W^- and outgoing lepton to the electron beam, and the shift in the peak position of the $W^\pm$ invariant-mass distributions. Disregarding the naive running-width scheme, it appears that only in the total cross-section one sees any effect of the different schemes. For most other quantities the deviations are less than the integration accuracies.

We now discuss the various schemes in a situation where U(1) electromagnetic gauge invariance is crucial. To this end we consider the cross-section for $e^-e^+ \to e^-\bar{\nu}_e u\bar{d}$ allowing for almost collinear incoming and outgoing electrons.[8] In Table 2 we give the total cross-section without canonical LEP2 cuts except for a beam-angle cut of the final-state electron to either beam ($\theta^{\min}_{e^-,\mathrm{beam}}$) for the typical LEP2 energy of $\sqrt{s} = 175$ GeV. Satisfactory agreement is found in general between ERATO and WWF although some discrepancy is present for small $\theta^{\min}_{e^-,\mathrm{beam}}$ in the running-width scheme owing to the unphysical $1/q_\gamma^4$ peak. Breaking U(1) gauge invariance clearly gives wrong results in the collinear region, as was already argued in Ref. [1].

In Table 3 we list the same cross-section as in Table 2, but now with canonical LEP2 cuts applied (the cut on the angle between the outgoing electron and either beam is still varied). This demonstrates that the U(1) violation is only related to collinear electrons and that, down to approximately 0.1°, there are no sizeable effects from including a cut on the energy of the outgoing electron (at least, compared with the expected experimental precision). This collinear behavior is made more pronounced in Fig. 1, where the cross-section without any cuts is shown as a function of the virtuality of the photon $[q_\gamma^2 = (p_2 - p_1)^2]$.

The deviations between the schemes other than the U(1)-violating running-width scheme are small. In adding the full fermionic contribution one observes nevertheless an increase in cross-section compared with the other U(1)-invariance-preserving schemes. At 10° ERATO/WWF give a result in the full

[7] WWF includes masses to the necessary approximation [20].

[8] If the angle between the incoming and outgoing electron is allowed to become arbitrarily small, the fermion masses in the loops and $\Gamma_\gamma^{f,\mu}$ can no longer be neglected.

$\theta^{\min}_{e^-,\text{beam}}$	0.1°	1°	10°
Running width	1.380(6)	0.6284(8)	0.5904(7)
	1.426(3)	0.6332(7)	0.5918(6)
Fixed width	0.6444(9)	0.6214(8)	0.5904(7)
	0.6443(3)	0.6210(3)	0.5909(2)
Running width	0.6448(9)	0.6219(8)	0.5912(7)
+ γWW vertex factor	0.6456(7)	0.6214(7)	0.5916(6)
Minimal FL scheme	0.6463(9)	0.6218(8)	0.5910(7)
Full FL scheme	0.6507(11)	0.6280(9)	0.6002(8)
	0.6514(9)	0.6298(7)	0.5992(7)

Table 2: Total cross-sections (in pb) for the CC20 process at $\sqrt{s} = 175$ GeV without ISR and without cuts except on the angle between the outgoing electron and either beam, as predicted by ERATO (first entry) and by WWF (second entry).

$\theta^{\min}_{e^-,\text{beam}}$	0.1°	0.5°	1°	5°	10°
Running width	1.36(1)	0.654(3)	0.6249(4)	0.60167(6)	0.58907(5)
Fixed width	0.641(1)	0.6256(8)	0.6188(5)	0.6020(2)	0.58915(5)
Running width + γWW vertex factor	0.641(1)	0.6245(5)	0.6187(5)	0.60190(2)	0.589242(8)
Full FL scheme	0.642(3)	0.630(1)	0.6247(4)	0.6100(2)	0.59771(7)

Table 3: Total cross-sections (in pb) for the CC20 process at $\sqrt{s} = 175$ GeV with the default setup except for a variable cut on the angle between the outgoing electron and either beam, as predicted by WTO.

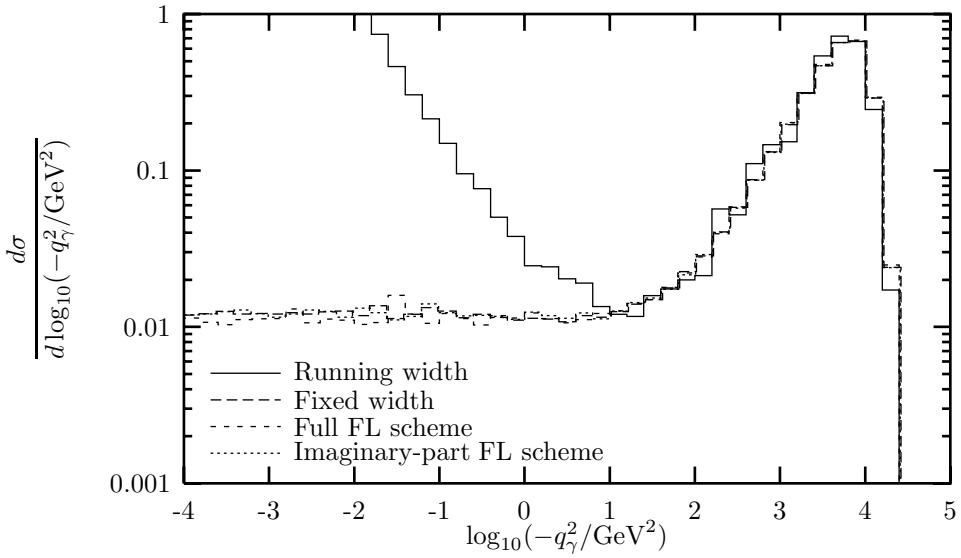

Figure 1: The effect of gauge-breaking terms in the CC20 process at $\sqrt{s} =$ 175 GeV as a function of the virtuality q_γ^2 of the photon without ISR and without cuts, as predicted by WWF.

FL scheme which is 1.7%/1.4% higher than the one obtained in the fixed-width scheme but the effect is decreasing at small scattering angles. This is not related to the collinear-electron limit, but is rather a direct consequence of the incorporation of the complete fermionic $\mathcal{O}(\alpha)$ effects, which are only partly taken into account in the other schemes by using improved Born couplings. In the full FL scheme the fermionic corrections enter via the universal running couplings, via the propagator functions $\chi_{W,Z}$, and via the vertex corrections.

For instance, the running of the couplings is such that between 100 and 1000 GeV they increase by several percent. This provides a qualitative estimate of the size of the fermionic corrections that are not included in the effective couplings Eq.(53). Because these couplings are fixed at the scale of the W- and Z-boson masses, this effect is small at LEP2 energies. However, the increase of the couplings as a function of p^2 will tend to increase the cross-section in the full FL scheme at high energies with respect to the other schemes. Of course, the neglected bosonic contributions will temper or even reverse the running of the couplings above the boson thresholds [in view of the asymptotic freedom of $g_w^2(p^2)$], so the computed values will in general be too high.

In Table 4 we present a more realistic calculation at three typical LEP2 energies: the total cross-section with ISR and canonical LEP2 cuts. The ISR has been implemented in the leading-logarithmic approximation, in the same way as it has been used for the tuned comparisons in Ref. [11]. The numbers

$\sqrt{s}$	161 GeV	175 GeV	190 GeV
Running width	0.1191(2)	0.4865(6)	0.6127(7)
Fixed width	0.1174(2)	0.4862(6)	0.6124(6)
Running width + γWW vertex factor	0.1192(2)	0.4864(6)	0.6125(7)
Minimal FL scheme	0.1191(2)	0.4864(6)	0.6128(7)
Full FL scheme	0.1208(3)	0.4930(7)	0.6220(6)
Running width	0.11942(3)	0.48681(4)	0.6135(7)
Fixed width	0.11764(3)	0.48674(4)	0.61314(9)
Running width + γWW vertex factor	0.11941(3)	0.48690(4)	0.6136(7)
Imaginary-part FL scheme	0.1195(2)	0.4861(3)	0.6125(9)
Full FL scheme	0.1215(2)	0.4934(3)	0.6223(9)
Running width	0.1195(2)	0.4878(6)	0.6119(7)
Fixed width	0.11757(5)	0.48636(16)	0.61271(22)
Running width + γWW vertex factor	0.1196(2)	0.4875(6)	0.6138(8)
Full FL scheme	0.1213(2)	0.4946(6)	0.6229(8)

Table 4: Total cross-sections (in pb) for the CC20 process at LEP2 energies with ISR and canonical cuts, as predicted by ERATO (rows 1–5), WTO (rows 6–10) and WWF (rows 11–14).

from the various generators agree rather well.

The difference between the minimal FL scheme (implemented in ERATO) and the imaginary-part FL scheme (implemented in WTO) is approximately 0.3% at $\sqrt{s} = 161\,\mathrm{GeV}$ and below 0.1% above threshold, thus at the level of (or below) the integration errors. Technically the imaginary-part FL scheme is obtained from the full FL scheme when all non-imaginary corrections are set to zero, however, the most relevant universal (real) corrections are accounted for by fixing α as in Eq.(53), giving a satisfactory agreement with the minimal approach. As for the full FL predictions, the differences between the three programs are always below 0.6%. On threshold, the fixed-width scheme underestimates the cross-section by 1.4–1.6% compared with the other schemes.

In adding the full fermionic contribution one observes a 1.6% increase in cross-section at the W-pair threshold, compared with the other schemes. The deviation remains practically constant up to 190 GeV. Comparing the values at

$\sqrt{s}$	200 GeV	500 GeV	1 TeV	2 TeV	5 TeV	10 TeV
Running width	672.96(3)	225.45(3)	62.17(1)	33.06(1)	123.759(8)	481.18(5)
	673.1(6)	225.5(3)	62.17(10)	33.05(4)	123.75(8)	485.7(3)
Fixed width	673.08(4)	224.05(3)	56.90(1)	13.19(1)	2.212(6)	0.591(4)
	673.3(6)	224.2(3)	56.93(10)	13.17(3)	2.209(10)	0.584(5)
Imaginary-part FL scheme	673.1(1)	224.5(7)	56.8(1)	13.18(4)	2.24(3)	0.597(6)
Minimal FL scheme	672.7(6)	223.9(3)	56.85(10)	13.09(4)	2.215(11)	0.584(5)
Full FL scheme	683.7(1)	227.9(2)	58.0(1)	13.57(4)	2.34(3)	0.632(6)
	685.0(6)	228.1(3)	57.89(9)	13.59(4)	2.290(11)	0.621(5)

Table 5: Total cross-sections (in fb) for the CC10 process at high energies (default setup), as predicted by WTO (first entry) and ERATO (second entry).

$\sqrt{s}$	200 GeV	500 GeV	1 TeV	2 TeV
Running width	2.0395(1)	0.8113(2)	0.3254(2)	0.1671(9)
Fixed width	2.0399(1)	0.8072(2)	0.3096(2)	0.1075(9)
Imaginary-part FL scheme	2.0397(5)	0.8067(9)	0.3087(8)	0.1073(8)
Full FL scheme	2.0720(3)	0.8212(9)	0.3145(8)	0.1097(9)

Table 6: Total cross-sections (in pb) for the CC11 process at high energies (default setup), as predicted by WTO.

$\sqrt{s} = 175$ GeV for the case with and without ISR, the cross-section is seen to decrease by approximately 17%, which is reasonable since we are close to the W-pair threshold and ISR lowers the effective s.

In order to study the effects of SU(2) violation we have to consider high energies. These effects are present in all processes that involve the W-pair-production diagrams. In Tables 5 and 6 we give the cross-sections for the processes CC10 and CC11, respectively. The quality of agreement between ERATO and WTO is satisfactory, with perhaps some marginal discrepancy for the running-width scheme at the highest energy. The cross-section for CC11 is larger by about a factor three owing to the color factor. From these results it is clear that for large s the fixed-width scheme and the FL schemes yield

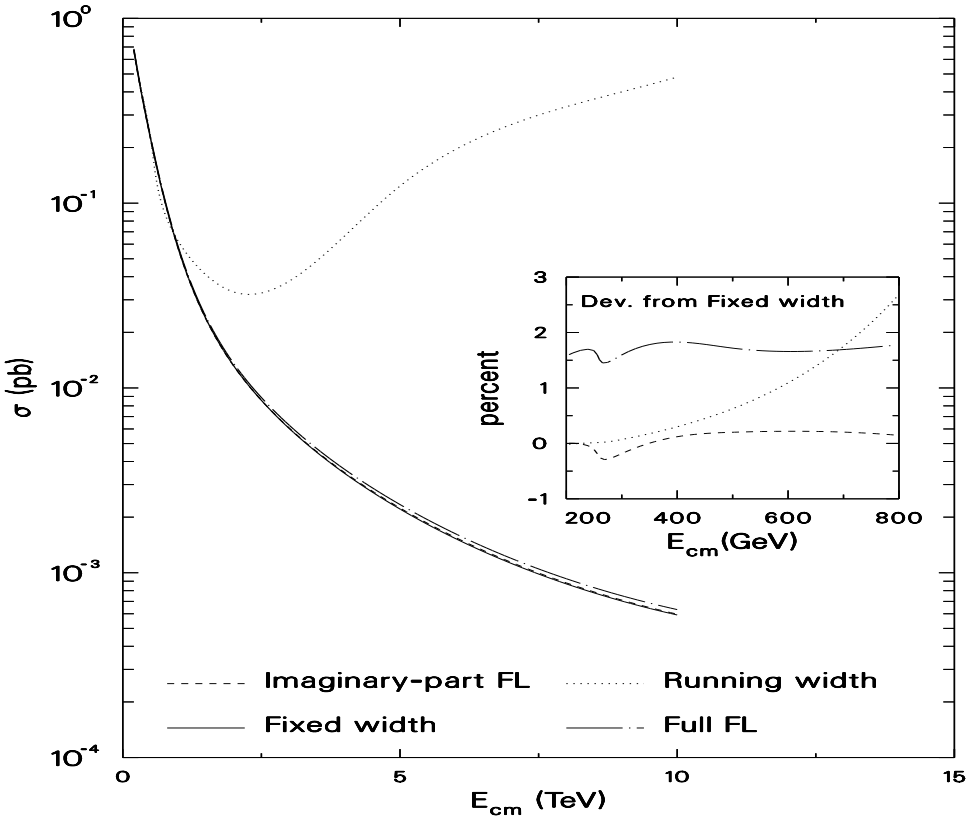

Figure 2: Total cross-sections for the CC10 process (default setup), as predicted by WTO, and deviations of the various schemes with respect to the fixed-width scheme in percent.

reasonable results, whereas the running-width scheme diverges. The latter deviates already at 1 TeV significantly and yields wrong results at higher energies. The fixed-width scheme and the imaginary-part FL scheme agree within $2\,\sigma$ (thus at the percent level) up to high energies. Although both the fixed-width scheme and FL schemes respect unitarity for large s, only the FL schemes satisfy SU(2) gauge invariance. As mentioned above, the gauge-invariance-violating terms that are introduced by the fixed-width scheme in the cross-sections for $e^-e^+ \to 4f$ are only of order $\mathcal{O}(m\Gamma/s)$. Therefore, the high-energy behavior in six-fermion processes is consistent with unitarity, although gauge invariance is broken.

At energies above 1 TeV the full FL scheme deviates from the fixed-width scheme and the minimal (imaginary-part) FL scheme by 1.7–6.3% (1.9–6.9%), according to ERATO (WTO). Note that this is just the order of magnitude that is to be expected from the running of the couplings. This rather large effect should be interpreted with care owing to the omission of QCD and bosonic corrections.

The high-energy behavior of the different schemes as predicted by WTO is

$\sqrt{s}$	200 GeV	500 GeV	1 TeV	2 TeV	10 TeV
Running width	0.7058(10)	0.3728(11)	0.2751(17)	0.2163(19)	0.5135(10)
	0.7070(4)	0.374(1)	0.281(4)		
Fixed width	0.7062(8)	0.3734(11)	0.2709(17)	0.1965(19)	0.0305(6)
	0.70719(6)	0.372(1)	0.275(4)		
Running width + γWW vertex factor	0.7045(10)	0.3736(11)	0.2763(17)	0.2176(19)	0.5261(10)
Minimal FL scheme	0.7060(6)	0.3713(11)	0.2705(17)	0.2000(19)	0.0306(6)
Full FL scheme	0.7177(7)	0.3776(11)	0.2797(17)	0.2076(22)	0.0326(6)
	0.7186(3)	0.377(5)	0.280(9)		

Table 7: Total cross-sections (in pb) for the CC20 process at high energies (default setup), as predicted by ERATO (first entry) and, in the NLC energy range, by WTO (second entry).

also shown in Fig. 2 for the CC10 cross-section. In the same figure we have illustrated the behavior of the corrections in a region of energy accessible to the NLC. Deviations from the fixed-width results are given, showing the $\bar{t}t$ threshold at approximately 264 GeV and the relatively minor impact of the imaginary-part FL scheme. In the whole range of energy between 200 GeV and 1 TeV the imaginary-part FL scheme deviates by less than 0.3% (only reached around the $\bar{t}t$ threshold) from the fixed-width scheme.

Since the running-width scheme reaches a 9.3% deviation in the same region, we may conclude that the imaginary-part FL scheme offers here the same quantitative behavior as the fixed-width calculation, but within a fully self-consistent approach. So does the minimal FL scheme, at least away from the $\bar{t}t$ threshold (where the top-mass effects play a role).

We register a difference between running-width and fixed-width results of 9.3% (CC10) and 5.1% (CC11) at 1 TeV. So, a gauge-invariance-preserving scheme is of actual relevance already for the NLC, and not only for theoretical speculations at extremely high energies. Moreover, a realistic estimate of the radiative corrections—within 1% accuracy—in the phenomenologically interesting region cannot avoid the proper inclusion of the bosonic corrections.

In Table 7 we list the total cross-section for the process $e^-e^+ \to e^-\bar{\nu}_e u\bar{d}$ at NLC and higher energies. The predictions by ERATO have been confirmed in the NLC energy region by WTO within the integration errors. This table shows the same features that were already discussed for CC10/11 before. The cross-section of this process is more sizeable than that of the CC10 process owing to

the presence of photonic t-channel diagrams. The relative importance of the W-pair-production diagrams is suppressed and therefore the bad high-energy behavior of the running-width schemes, which originates from these diagrams, occurs at higher energies. Note that also the running-width scheme with the U(1)-invariance-preserving γWW-vertex factor diverges.

The net effect of the full FL scheme is quite large, reaching 5.6% at 2 TeV and 6.9% at 10 TeV. This effect can be understood by noticing that in the fixed-width scheme we use G_F everywhere (except for ISR). In the TeV range the t-channel photon-exchange contributions become dominant and in Born approximation these diagrams are evaluated for $\alpha^{-1} = 131.2$. In the full FL scheme α is effectively replaced by $\alpha(|t_{min}|) = \alpha(s\,[1-\cos(10^\circ)]/2)$, which is larger ($\alpha^{-1} = 131.2$ roughly corresponds to $q^2 = [18\,\mathrm{GeV}]^2$). A rough estimate of the effect gives $[\alpha(|t_{min}|)/131.2]^2 \approx 1.050, 1.090$ for $2, 10$ TeV.

5 Conclusions

In Ref. [1] we had introduced the fermion-loop (FL) scheme for the gauge-invariant treatment of the finite-width effects of W and Z bosons. This scheme consists in including all fermionic one-loop corrections in tree-level amplitudes and resumming the self-energies. In this article we have presented the justification and an extension of the FL scheme. We have performed the full resummation and renormalization of the fermionic one-loop corrections to six-fermion processes, including virtual massive top-quark effects and ε-tensor contributions. A simple *effective Born* prescription has been presented, which allows for a relatively straightforward implementation of the full fermionic one-loop corrections to LEP2 six-fermion processes. We have given explicit formulae that are sufficient for all such non-QCD processes and discussed the gauge invariance of the amplitudes. We have implemented the full FL scheme in three different Monte-Carlo generators, which were used to compute the cross-section for the processes $e^-e^+ \to \mu^-\bar\nu_\mu u\bar d$, $e^-e^+ \to s\bar c u\bar d$, and $e^-e^+ \to e^-\bar\nu_e u\bar d$, and we have compared the results with other schemes, including simplified variants of the full FL scheme.

The fixed-width and FL schemes behave properly in the collinear and high-energy regions of phase space, as required. The other schemes are seen to diverge for large s. It should be noted, however, that only the FL schemes satisfy SU(2) gauge invariance. The gauge-invariance-violating terms in the fixed-width scheme are suppressed for large s in six-fermion processes. For processes with more intermediate gauge bosons the fixed-width scheme gives rise to a bad high-energy behavior.

In order to include the finite width into tree-level matrix elements it is sufficient to use a minimal subset of the fermionic corrections given by the imaginary parts of the fermion loops for massless fermions. This significantly simplifies the expressions and increases the speed of the computation. Moreover, in practical LEP2 calculations it is even sufficient to use running widths and to supplement these by incorporating the imaginary parts of the fermionic one-loop corrections

to the γWW vertex in the limit $q_\gamma^2 \to 0$.

In contrast to the schemes that are only based on the imaginary parts of the fermion loops the full FL scheme includes the complete fermionic $\mathcal{O}(\alpha)$ corrections. Indeed, the full FL scheme can be viewed as a first attempt to include all $\mathcal{O}(\alpha)$ radiative corrections. As a consequence, the corresponding results differ from the ones obtained with the other schemes by some percent at LEP2, and much more for higher energies. To give an idea of this effect we consider our most complete set of predictions, i.e., the CC20 process with ISR at $\sqrt{s} = 161\,\text{GeV}, 175\ \text{GeV}$ and $190\,\text{GeV}$. The difference amounts to approximately 1.3–1.6%. At higher (NLC) energies (up to 2 TeV) the differences range from 1.6–2.0% for CC11 to 1.5–3% for CC10 and 1–5% for CC20. This is a non-negligible effect from the experimental point of view. Once more we stress that the relatively large effects induced by the full FL scheme should be interpreted with due caution.

The full FL scheme, including the fermionic corrections with resummation, already has some of the features that the ultimate event generator should have. Therefore it represents a justification of the scheme of Ref. [1] and a starting point for the evaluation of all $\mathcal{O}(\alpha)$ radiative corrections in a situation where we know that the impact of the bosonic corrections cannot be neglected. It is therefore important to know the bosonic one-loop corrections and to see whether the increase in the cross-section owing to the fermionic corrections is significant for experiments. Inclusion of the bosonic one-loop corrections will possibly temper the increase, in particular at high energies. The large impact of the bosonic corrections is mainly due to corrections of the form $\alpha/\pi \log^2(s/m_W^2)$ as explicitly calculated for on-shell W bosons. Another large part of the bosonic corrections, as e.g. the leading-logarithmic corrections (initial-state radiation), factorizes and can be treated by a convolution. A proper treatment of the complete bosonic one-loop corrections is still lacking.

Simultaneous inclusion of bosonic corrections and finite-width effects leads in general to problems with gauge invariance. Manifestly gauge-independent amplitudes can be obtained upon an expansion about the complex pole. This so-called pole scheme is based on a systematic expansion according to the degree of resonance and thus allows an efficient calculation of the most important higher-order corrections. However, one version of the pole scheme is only applicable sufficiently far above the W-pair production threshold, whereas other versions do not preserve the SU(2) Ward identities (for the same reason as the fixed-width scheme).

A direct generalization of the FL scheme to the complete (fermionic and bosonic) corrections is provided by the background-field formalism, where Ward identities hold also after Dyson summation. However, also in this formalism the Dyson summation introduces a gauge dependence, starting at the loop level which is not completely taken into account. This gauge dependence is nothing but a reflection of the fact that any resummation is arbitrary to some extent.

Another possibility would be to use a hybrid scheme, i.e., using the FL scheme and adding the bosonic corrections by means of the pole scheme. In any case, the proper inclusion of the bosonic corrections needs further investigation.

Note added

Shortly before finishing this paper a preprint related to our work appeared [21]. In this paper the absorptive part of the γWW vertex is evaluated for massive fermions and the photon on shell. It is stressed that the axial contribution of this vertex is not zero. We would like to emphasize that this is not in contradiction to our previous work [1]. In Ref. [1] we restricted ourselves to massless fermions and even issued a warning that (massive) top-quark effects were not included. Moreover, as the axial contribution satisfies the Ward identities on its own it is not required for a gauge-invariant description of finite-width effects. Once the axial contribution is taken into account the non-absorptive parts should be included as well: then one arrives at the full fermion-loop scheme that we are presenting in this paper.

Acknowledgments

This research has been partly supported by the EU under contract numbers CHRX-CT-92-0004, CHRX-CT-93-0319, and CHRX-CT-94-0579. W. Beenakker is supported by a fellowship of the Royal Dutch Academy of Arts and Sciences. G.J. van Oldenborgh, J. Hoogland and R. Kleiss are supported by FOM. C.G. Papadopoulos would like to thank the Department of Physics of the University of Durham, UK, where part of this work was done, for its kind hospitality. G. Passarino gratefully acknowledges the help of A. Ballestrero and R. Pittau in several comparisons performed during this work. We would also like to thank the CERN Liquid Support Division.

A Gauge-boson self-energies

In this appendix we give explicit formulae for the fermionic one-loop contributions to the gauge-boson self-energies. First we give the results for arbitrary fermion masses, subsequently we take the limit $m_f \to 0$ for $f \neq t$. The electric charge fraction of the fermion f is denoted by Q_f, its vector and axial-vector couplings to the Z boson by v_f and a_f, its iso-spin by I_f^3, its left-handed hypercharge by $Y_f^L = 2(Q_f - I_f^3)$ [-1 for leptons and $1/3$ for quarks], and its color factor by N_c^f.

We do not include tadpole contributions, i.e., we implicitly assume that the tadpoles are removed by appropriate counter terms.

The fermionic contributions to the photon self-energy and photon–Z mixing energy read

$$\begin{aligned}
\hat{\Sigma}_\gamma(p^2) &= \frac{\hat{\alpha}}{3\pi} \sum_f N_c^f \, Q_f^2 \left\{ p^2 \left[B_0(p^2,0,0) - \frac{1}{3} \right] + F(p^2, m_f) \right\}, \\
\hat{\Sigma}_{\gamma Z}(p^2) &= -\frac{\hat{\alpha}}{3\pi} \sum_f N_c^f \, \hat{v}_f Q_f \left\{ p^2 \left[B_0(p^2,0,0) - \frac{1}{3} \right] + F(p^2, m_f) \right\}, \quad (54)
\end{aligned}$$

where $\hat{\alpha} = \hat{e}^2/(4\pi)$, B_0 is the one-loop scalar 2-point function [10], and

$$F(p^2, m_f) = (p^2 + 2m_f^2)\, B_0(p^2, m_f, m_f) - 2m_f^2\, B_0(0, m_f, m_f) - p^2\, B_0(p^2, 0, 0)\ . \tag{55}$$

The function $F(p^2, m_f)$ is finite and vanishes for $m_f = 0$ as well as for $p^2 = 0$. For $|p^2| \ll m_f^2$ we obtain for $\hat{\Pi}_\gamma(p^2) \equiv \hat{\Sigma}_\gamma(p^2)/p^2$

$$\hat{\Pi}_\gamma(p^2) \approx \frac{\hat{\alpha}}{3\pi} \sum_f N_c^f\, Q_f^2 \left[B_0(0, m_f, m_f) + \frac{p^2}{5m_f^2} \right] . \tag{56}$$

The running of the coupling is given by

$$p^2 \frac{\partial}{\partial p^2} \frac{\hat{\alpha}}{\alpha(p^2)} = p^2 \frac{\partial}{\partial p^2} \hat{\Pi}_\gamma(p^2) \stackrel{p^2 \to 0}{\longrightarrow} 0\ . \tag{57}$$

As a result of the decoupling, the fermion f does not contribute to the p^2 evolution of the running electromagnetic coupling $\alpha(p^2)$ if $|p^2| \ll m_f^2$. Hence, the masses of the light fermions cannot be neglected for very low momentum transfers, $|p^2| \lesssim m_f^2$, as is the case for near-collinear photon emission from light particles.

The fermionic contributions to the Z and W self-energies are given by Eq.(2) with

$$\begin{aligned}
\hat{\overline{\Sigma}}_Z(p^2) &= \frac{\hat{\alpha}}{3\pi} \sum_f N_c^f \left\{ (\hat{v}_f^2 + \hat{a}_f^2)\, p^2 \left[B_0(p^2, 0, 0) - \frac{1}{3} \right] \right. \\
&\qquad \left. + (\hat{v}_f^2 + \hat{a}_f^2 + 4 I_f^3 Y_f^L \hat{a}_f^2)\, F(p^2, m_f) \right\} , \\
\hat{\overline{\Sigma}}_W(p^2) &= \frac{\hat{g}_w^2}{48\pi^2} \sum_f N_c^f \left\{ p^2 \left[B_0(p^2, 0, 0) - \frac{1}{3} \right] + (1 + 2 I_f^3 Y_f^L)\, F(p^2, m_f) \right\} ,
\end{aligned} \tag{58}$$

and

$$\begin{aligned}
T_z(p^2) &= -\sum_f \frac{N_c^f}{48\pi^2} \left[3m_f^2\, B_0(p^2, m_f, m_f) + 2 I_f^3 Y_f^L\, F(p^2, m_f) \right] , \\
T_w(p^2) &= T_z(p^2) + \sum_{\text{doublets}} \frac{N_c^f}{48\pi^2} \left\{ \left(2p^2 - m_f^2 - m_{f'}^2\right) B_0(p^2, m_f, m_{f'}) \right. \\
&\quad - (p^2 - m_f^2)\, B_0(p^2, m_f, m_f) - (p^2 - m_{f'}^2)\, B_0(p^2, m_{f'}, m_{f'}) \\
&\quad + \frac{m_f^2 - m_{f'}^2}{p^2} \left[m_f^2\, B_0(0, m_f, 0) - m_{f'}^2\, B_0(0, m_{f'}, 0) \right. \\
&\qquad \left. \left. + (m_{f'}^2 - m_f^2)\, B_0(p^2, m_f, m_{f'}) \right] \right\} .
\end{aligned} \tag{59}$$

Here (f, f') represent the iso-spin partners within an SU(2) doublet. The terms involving $F(p^2, m_f)$ in $\hat{\overline{\Sigma}}_Z$ and $\hat{\overline{\Sigma}}_W$ are determined such that the relations Eq.(3), which hold for massless fermions, hold also in the massive case. At zero momentum transfer the Z and W self-energies are given by the non-universal terms only:

$$\begin{aligned}
\frac{\hat{\Sigma}_Z(0)}{\hat{\mu}_z} = \frac{\hat{g}_w^2\, T_Z(0)}{\hat{c}_w^2\, \hat{\mu}_z} &= -\sum_f \frac{\hat{g}_w^2}{16\pi^2 \hat{c}_w^2}\, N_c^f\, \frac{m_f^2}{\hat{\mu}_z}\, B_0(0, m_f, m_f)\,, \\
\frac{\hat{\Sigma}_W(0)}{\hat{\mu}_W} = \frac{\hat{g}_w^2\, T_W(0)}{\hat{\mu}_W} &= -\sum_f \frac{\hat{g}_w^2}{16\pi^2}\, N_c^f\, \frac{m_f^2}{\hat{\mu}_W} \left[B_0(0, m_f, m_f) + \frac{1}{2} \right. \\
&\qquad \left. + \frac{m_{f'}^2}{m_{f'}^2 - m_f^2} \log \frac{m_f}{m_{f'}} \right]. \qquad (60)
\end{aligned}$$

At momentum transfers of the order of the LEP1/2 energies the fermion masses can be neglected, with the exception of the top-quark mass. In this limit all contributions of the form $F(p^2, m_f)$ drop out for $f \neq t$ and the universal self-energies are proportional to the photon self-energy:

$$\begin{aligned}
\hat{\Sigma}_x(p^2) &= \frac{\hat{s}_w}{\hat{c}_w} \left(1 - \frac{3}{8\hat{s}_w^2} \right) \hat{\Sigma}_\gamma(p^2)\,, \\
\hat{\overline{\Sigma}}_z(p^2) &= \frac{\hat{s}_w^2}{\hat{c}_w^2} \left(1 - \frac{3}{4\hat{s}_w^2} + \frac{3}{8\hat{s}_w^4} \right) \hat{\Sigma}_\gamma(p^2)\,, \\
\hat{\overline{\Sigma}}_w(p^2) &= \frac{3}{8\hat{s}_w^2}\, \hat{\Sigma}_\gamma(p^2)\,. \qquad (61)
\end{aligned}$$

The non-universal contributions T_Z and T_W take on the form

$$\begin{aligned}
T_z(p^2) &= -\frac{N_c^t}{144\pi^2} \left[9m_t^2\, B_0(p^2, m_t, m_t) + F(p^2, m_t) \right], \\
T_w(p^2) &= \frac{N_c^t}{48\pi^2} \left[\left(2p^2 - m_t^2 - \frac{m_t^4}{p^2} \right) B_0(p^2, m_t, 0) \right. \\
&\qquad - \frac{4}{3} \left(p^2 + 2m_t^2 \right) B_0(p^2, m_t, m_t) - \frac{2}{3} p^2\, B_0(p^2, 0, 0) \\
&\qquad \left. + \frac{2}{3} m_t^2\, B_0(0, m_t, m_t) + \frac{m_t^4}{p^2}\, B_0(0, m_t, 0) \right]. \qquad (62)
\end{aligned}$$

At zero momentum transfer Eq.(60) simplifies to

$$\begin{aligned}
\frac{\hat{\Sigma}_Z(0)}{\hat{\mu}_z} = \frac{\hat{g}_w^2\, T_Z(0)}{\hat{c}_w^2\, \hat{\mu}_z} &= -\frac{\hat{g}_w^2}{16\pi^2 \hat{c}_w^2}\, N_c^t\, \frac{m_t^2}{\hat{\mu}_z}\, B_0(0, m_t, m_t)\,, \\
\frac{\hat{\Sigma}_W(0)}{\hat{\mu}_W} = \frac{\hat{g}_w^2\, T_W(0)}{\hat{\mu}_W} &= -\frac{\hat{g}_w^2}{16\pi^2}\, N_c^t\, \frac{m_t^2}{\hat{\mu}_W} \left[B_0(0, m_t, m_t) + \frac{1}{2} \right]. \qquad (63)
\end{aligned}$$

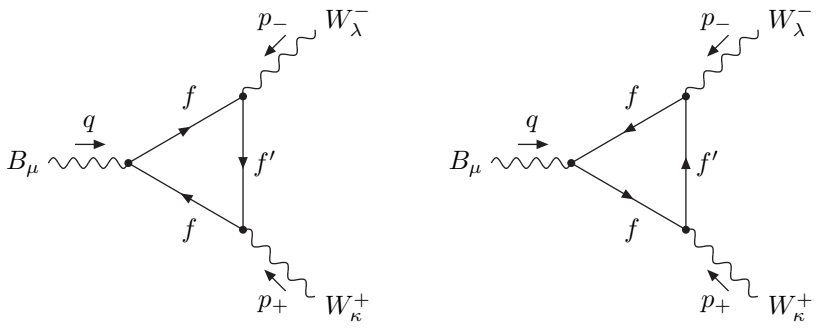

Figure 3: Feynman diagrams for the fermion-loop corrections to the BW^+W^- vertex ($B = \gamma, Z$). All particles are assumed to be incoming.

We note that when evaluating $B_0(\mu_{z,w}, m_1, m_2)$ care has to be taken, because the complex pole does not lie on the usual physical (first) Riemann sheet. Its location is determined by the fact that it should smoothly approach the value for a stable gauge boson when the coupling tends to zero.

B Fermion-loop corrections to the triple gauge-boson vertices

At one loop, the fermion-loop corrections to the triple gauge-boson vertices consist of two sets of contributions, which are generically depicted in the two diagrams in Fig. 3 for the vertices involving W bosons. In the diagram on the right-hand side f is a down-type fermion, in the one on the left-hand side f is up-type.

B.1 Vertices involving charged bosons

In this appendix we give the fermion-loop corrections to the ZWW and γWW vertex functions for arbitrary fermion masses. All results are presented in terms of one-loop tensor-integral coefficient functions:

$$
\begin{aligned}
&\hat{V}^{(1),\{\gamma,Z\}W^+W^-,\mu\kappa\lambda}(q,p_+,p_-) \;= \\
&\quad\left\{\frac{\hat{e}\hat{g}_w^2}{32\pi^2}\sum_f N_c^f\left[-|Q_f|\left\{1,-\frac{\hat{c}_w}{\hat{s}_w}\right\}+\frac{1-2|Q_f|}{2\hat{s}_w\hat{c}_w}\{0,1\}\right]\right. \\
&\quad\times\Big\{q^\mu g^{\kappa\lambda}\left[B_0(p_+^2)+p_+^2\,(C_0+C_1-C_2)-(q^2+2m_f^2+2m_{f'}^2)\,C_1+8\,C_{001}\right] \\
&\quad+(p_+-p_-)^\mu g^{\kappa\lambda}\left[-B_0(p_+^2)-q^2\,C_1\right.
\end{aligned}
$$

$$
\begin{aligned}
&\quad + (p_+^2 - m_f^2 - m_{f'}^2)\,(C_0 + C_1 + C_2) + 4\,C_{00} + 8\,C_{001}\Big] \\
&+ p_-^\lambda g^{\mu\kappa}\Big[2\,B_0(p_-^2) + 4\,B_1(p_-^2) - B_0(p_+^2) + B_0(q^2) \\
&\quad + (p_-^2 - 2p_+^2 + m_f^2 + m_{f'}^2)\,C_0 + (p_-^2 - p_+^2 - q^2)\,(2C_1 + C_2) \\
&\quad - 8\,C_{00} - 16\,C_{001} - 8\,C_{002}\Big] \\
&+ (q - p_+)^\lambda g^{\mu\kappa}\Big[-B_0(q^2) - B_0(p_+^2) \\
&\quad + (p_-^2 - m_f^2 - m_{f'}^2)\,C_0 + (p_-^2 - p_+^2 - q^2)\,C_2 - 8\,C_{002}\Big] \\
&- q^\mu p_+^\kappa p_-^\lambda\, 2\,[C_1 + 3\,C_{11} + 2\,C_{111} + 3\,C_{112}] \\
&- (p_+ - p_-)^\mu p_+^\kappa p_-^\lambda\,[6\,C_1 + 10\,C_{11} + 11\,C_{12} + 4\,C_{111} + 14\,C_{112}] \\
&- q^\mu p_+^\kappa (q - p_+)^\lambda\, 2\,[C_2 + C_{12} - C_{22} + C_{112} + C_{122} - 2\,C_{222}] \\
&- q^\mu (q - p_+)^\lambda (q - p_-)^\kappa\, 2\,C_{112} \\
&- (p_+ - p_-)^\mu p_-^\lambda (q - p_-)^\kappa\, 2\,[C_1 + 3\,C_{11} + 2\,C_{12} + 2\,C_{111} + 3\,C_{112} + C_{122}] \\
&- (p_+ - p_-)^\mu (q - p_+)^\lambda (q - p_-)^\kappa\,[C_{12} + C_{112} + C_{122}]\Big\} \\
&+ \quad (p_+ \leftrightarrow -p_-,\, q \to -q,\, \kappa \leftrightarrow \lambda)\quad \Big\} \\
&+ \Big\{\frac{\hat{e}\hat{g}_w^2}{32\pi^2}\sum_f N_c^f\,\frac{1}{\hat{s}_w\hat{c}_w}\,\{0,1\}\,m_f^2\Big[q^\mu g^{\kappa\lambda}\,C_1 + (p_+ - p_-)^\mu g^{\kappa\lambda}\,C_1 \\
&+ p_-^\lambda g^{\mu\kappa}\,(2\,C_1 + C_2) + (q - p_+)^\lambda g^{\mu\kappa}\,C_2\Big] \\
&+ \quad (p_+ \leftrightarrow -p_-,\, q \to -q,\, \kappa \leftrightarrow \lambda)\quad \Big\} \\
&+ \frac{\hat{e}\hat{g}_w^2}{16\pi^2}\sum_f N_c^f\,\Big[-Q_f\,\Big\{1, -\frac{\hat{c}_w}{\hat{s}_w}\Big\} + \frac{I_f^3 - Q_f}{\hat{s}_w\hat{c}_w}\,\{0,1\}\Big] \\
&\times\Big\{i\varepsilon^{\mu\lambda\alpha\beta}p_-^\kappa p_{+,\alpha}p_{-,\beta}\,4\,C_{12} - i\varepsilon^{\mu\lambda\alpha\beta}p_+^\kappa p_{+,\alpha}p_{-,\beta}\,4\,[C_2 + C_{22}] \\
&- i\varepsilon^{\mu\kappa\alpha\beta}p_+^\lambda p_{+,\alpha}p_{-,\beta}\,4\,C_{12} + i\varepsilon^{\mu\kappa\alpha\beta}p_-^\lambda p_{+,\alpha}p_{-,\beta}\,4\,[C_1 + C_{11}] \\
&+ i\varepsilon^{\mu\kappa\lambda\alpha}q_\alpha\,\big[(p_+^2 + m_f^2 - m_{f'}^2)\,C_2 - (p_-^2 + m_f^2 - m_{f'}^2)\,C_1\big]\Big\} \\
&+ \frac{\hat{e}\hat{g}_w^2}{8\pi^2}\sum_f N_c^f\,\frac{I_f^3}{\hat{s}_w\hat{c}_w}\,\{0,1\}\,m_f^2\Big[-i\varepsilon^{\mu\kappa\lambda\alpha}p_{-,\alpha}\,C_1 + i\varepsilon^{\mu\kappa\lambda\alpha}p_{+,\alpha}\,C_2\Big]\,, \qquad (64)
\end{aligned}
$$

where m_f denotes the mass of the fermion that couples to the neutral gauge boson and $m_{f'}$ the mass of its iso-spin partner. The totally-antisymmetric ε-tensor is fixed according to $\varepsilon^{0123} = 1$. The conventions for the arguments of the tensor-integral coefficient functions C_{ijk} follow Ref. [9],

$$\begin{aligned} B_i(q^2) &= B_i(q, m_f, m_f) \,, \qquad B_i(p_\pm^2) = B_i(p_\pm, m_{f'}, m_f) \,, \\ C_{ijk} &= C_{ijk}(p_-, -p_+, m_{f'}, m_f, m_f) \,. \end{aligned} \tag{65}$$

In Eq.(64) the substitution ($p_+ \leftrightarrow -p_-$, $q \to -q$) also applies to the arguments of the tensor coefficients. For the C_{ijk}, C_{ij}, and C_i this is equivalent to the interchange of "1" and "2" in the indices, leaving the arguments unaffected.

From the above expression for $\hat{V}^{(1),\,\{\gamma,Z\}W^+W^-}$ one can easily read off the one-loop coefficients $G^{\gamma,\,(1)}$ and $G^{I,\,(1)}$. The UV divergence contained in $\hat{V}^{(1)}$ can be written as

$$\begin{aligned} \hat{V}^{(1),\,\{\gamma,Z\}W^+W^-}_{\mu\kappa\lambda}(q, p_+, p_-) &= \frac{\hat{e}\hat{g}_w^2}{48\pi^2} \left\{1, -\frac{\hat{c}_w}{\hat{s}_w}\right\} \Gamma_{\mu\kappa\lambda}(q, p_+, p_-) \sum_f N_c^f \, B_0(q^2) \\ &\qquad + \text{UV-finite terms} \\ &= \hat{e} \left\{1, -\frac{\hat{c}_w}{\hat{s}_w}\right\} \frac{\hat{\overline{\Sigma}}_W(q^2)}{q^2} \Gamma_{\mu\kappa\lambda}(q, p_+, p_-) + \text{UV-finite terms} \,, \end{aligned} \tag{66}$$

with $\Gamma_{\mu\kappa\lambda}$ defined in Eq.(32).

The vertex correction $\hat{V}^{(1)}$ contains ε-terms, which contribute to the triangle anomaly. The cancellation of the anomaly requires the contribution of the massive top quark. Writing

$$\hat{V}^{(1)} = \sum_f \hat{V}_f^{(1)}(m_f = 0) + \left[\hat{V}_{\text{top}}^{(1)}(m_t \neq 0) - \hat{V}_{\text{top}}^{(1)}(m_t = 0)\right], \tag{67}$$

it follows from the anomaly-cancellation conditions that all ε-terms disappear in the (massless) sum on the right-hand side. The remainder contains ε-terms and is m_t-dependent. This m_t dependence is known to produce effects of delayed unitarity cancellation, which may become relevant at high energies.

Introducing the auxiliary projective momenta and tensors

$$\begin{aligned} \bar{q}^\mu &= \frac{1}{q^2}\Big[(qp_-)p_+^\mu - (qp_+)p_-^\mu\Big] \,, \qquad & \bar{g}_0^{\kappa\lambda} &= g^{\kappa\lambda} - \frac{p_+^\lambda p_-^\kappa}{(p_+p_-)} \,, \\ \bar{p}_\pm^\nu &= p_\mp^\nu - \frac{(p_+p_-)}{p_\pm^2} p_\pm^\nu \,, & \bar{g}_\pm^{\mu\nu} &= g^{\mu\nu} - \frac{q^\nu p_\mp^\mu}{(qp_\mp)} \,, \end{aligned} \tag{68}$$

the terms in Eq.(64) involving no ε-tensors can be rewritten in the following way

$$\begin{aligned} \hat{V}^{(1),\,\{\gamma,Z\}W^+W^-,\,\mu\kappa\lambda}(q, p_+, p_-) &= q^\mu p_+^\kappa p_-^\lambda X_{0+-} + \bar{q}^\mu \bar{p}_+^\kappa \bar{p}_-^\lambda X^{0+-} \\ &\quad + \bar{q}^\mu p_+^\kappa p_-^\lambda X^0_{+-} + q^\mu p_+^\kappa \bar{p}_-^\lambda X^-_{0+} + q^\mu \bar{p}_+^\kappa p_-^\lambda X^+_{0-} \end{aligned}$$

$$
\begin{aligned}
&+ q^\mu \bar{p}_+^\kappa \bar{p}_-^\lambda X_0^{+-} + \bar{q}^\mu p_+^\kappa \bar{p}_-^\lambda X_+^{0-} + \bar{q}^\mu \bar{p}_+^\kappa p_-^\lambda X_-^{0+} \\
&+ q^\mu \bar{g}_0^{\kappa\lambda} X_0 + p_+^\kappa \bar{g}_+^{\mu\lambda} X_+ + p_-^\lambda \bar{g}_-^{\mu\kappa} X_- \\
&+ \bar{q}^\mu \bar{g}_0^{\kappa\lambda} X^0 + \bar{p}_+^\kappa \bar{g}_+^{\mu\lambda} X^+ + \bar{p}_-^\lambda \bar{g}_-^{\mu\kappa} X^- \\
&+ \text{terms with } \varepsilon\text{-tensors}
\end{aligned} \tag{69}
$$

with appropriate coefficient functions X. The covariants introduced in Eq.(68) are constructed such that

$$
\begin{aligned}
(q\bar{q}) \;&=\; 0, \qquad & (p_\pm \bar{p}_\pm) &= 0, \\
p_+^\kappa\, \bar{g}_{0,\kappa\lambda} = p_-^\lambda\, \bar{g}_{0,\kappa\lambda} \;&=\; 0, \qquad & q^\mu\, \bar{g}_{\pm,\mu\nu} = p_\mp^\nu\, \bar{g}_{\pm,\mu\nu} &= 0.
\end{aligned} \tag{70}
$$

This implies that for a given external leg the "barred" quantities in $\hat{V}^{(1),\mu\kappa\lambda}$ drop out upon contraction with the corresponding momentum, e.g. $\bar{q}^\mu$ and $\bar{g}_\pm^{\mu\nu}$ vanish after contraction with q_μ. Hence the barred terms are not required for the restoration of the Ward identities; this must be done by the "unbarred" terms. On the other hand, each unbarred term contains at least one factor that vanishes upon contraction with a conserved current. At first sight, this situation looks paradoxical: the terms that restore gauge invariance do not explicitly contribute to the amplitude. However, the decomposition becomes singular for $q^2/E_{CM}^2 \to 0$, $p_\pm^2/E_{CM}^2 \to 0$, and as a result of the analyticity of the amplitudes barred and unbarred terms are related in these limits. But these limits correspond exactly to the kinematic situations where the Ward identities are required to guarantee well-behaved amplitudes.

B.2 Vertices involving only neutral bosons

In this appendix we give the fermion-loop contributions to the (C–odd and CP–even) triple gauge-boson vertices involving only neutral gauge bosons, which do not exist at lowest order. For each fermion the two diagrams of Fig. 3 with $f' = f$ contribute, and all terms cancel apart from those involving ε-tensors. We find for the generic, finite $B_1B_2B_3$ vertex ($B_i = \gamma, Z$):

$$
\begin{aligned}
\hat{V}^{(1),\,\mu\kappa\lambda}_{B_1B_2B_3}(q_1,q_2,q_3) \;&=\; \frac{\hat{e}^3}{8\pi^2} \sum_f N_c^f\, \hat{a}_{123}^{+++} \\
&\times \Big\{ i\varepsilon^{\mu\lambda\alpha\beta} q_3^\kappa q_{2,\alpha} q_{3,\beta}\, 4\, C_{12} - i\varepsilon^{\mu\lambda\alpha\beta} q_2^\kappa q_{2,\alpha} q_{3,\beta}\, 4\, [C_2 + C_{22}] \\
&- i\varepsilon^{\mu\kappa\alpha\beta} q_2^\lambda q_{2,\alpha} q_{3,\beta}\, 4\, C_{12} + i\varepsilon^{\mu\kappa\alpha\beta} q_3^\lambda q_{2,\alpha} q_{3,\beta}\, 4\, [C_1 + C_{11}] \\
&- i\varepsilon^{\mu\kappa\lambda\alpha} q_{3,\alpha} \left[(2m_f^2 - q_3^2)\, C_1 + q_2^2\, C_2 \right] \\
&+ i\varepsilon^{\mu\kappa\lambda\alpha} q_{2,\alpha} \left[(2m_f^2 - q_2^2)\, C_2 + q_3^2\, C_1 \right] \Big\} \\
&+ \frac{\hat{e}^3}{4\pi^2} \sum_f N_c^f\, m_f^2\, \hat{a}_{123}^{-++} \left[i\varepsilon^{\mu\kappa\lambda\alpha} q_{3,\alpha}\, C_1 - i\varepsilon^{\mu\kappa\lambda\alpha} q_{2,\alpha}\, C_2 \right]
\end{aligned}
$$

$$+\frac{\hat{e}^3}{4\pi^2}\sum_f N_c^f\, m_f^2\, \hat{a}_{123}^{+-+}\left[i\varepsilon^{\mu\kappa\lambda\alpha} q_{3,\alpha}\,(C_0+C_1) - i\varepsilon^{\mu\kappa\lambda\alpha} q_{2,\alpha}\, C_2\right]$$

$$+\frac{\hat{e}^3}{4\pi^2}\sum_f N_c^f\, m_f^2\, \hat{a}_{123}^{++-}\left[i\varepsilon^{\mu\kappa\lambda\alpha} q_{3,\alpha}\, C_1 - i\varepsilon^{\mu\kappa\lambda\alpha} q_{2,\alpha}\,(C_0+C_2)\right], \tag{71}$$

with

$$C_{ij} = C_{ij}(q_3, -q_2, m_f, m_f, m_f)\,, \tag{72}$$

and

$$\begin{aligned}\hat{a}_{123}^{\sigma_1\sigma_2\sigma_3} = {} & (\hat{v}_f^{B_1}+\sigma_1\hat{a}_f^{B_1})(\hat{v}_f^{B_2}+\sigma_2\hat{a}_f^{B_2})(\hat{v}_f^{B_3}+\sigma_3\hat{a}_f^{B_3}) \\ & -(\hat{v}_f^{B_1}-\sigma_1\hat{a}_f^{B_1})(\hat{v}_f^{B_2}-\sigma_2\hat{a}_f^{B_2})(\hat{v}_f^{B_3}-\sigma_3\hat{a}_f^{B_3})\,.\end{aligned} \tag{73}$$

The vector and axial-vector couplings $\hat{v}_f^{B_i}$ and $\hat{a}_f^{B_i}$ of the Z boson ($B_i = Z$) to fermions have been defined in Eq.(19), those of the photon ($B_i = \gamma$) to fermions are given by $\hat{a}_f^\gamma = 0$, $\hat{v}_f^\gamma = -Q_f$. As expected from the C-invariance of electromagnetic interactions, the $\gamma\gamma\gamma$ vertex function vanishes. The result for the Z-boson–gluon–gluon vertex can be obtained from the previous formulae by substituting $\hat{v}_f^{B_i} \to 1$, $\hat{a}_f^{B_i} \to 0$ for the gluon–fermion couplings and $\hat{e}^3 \to \hat{e} g_s^2 \delta^{ab}/2$, where g_s is the strong coupling constant, a and b the colors of the gluons, and δ^{ab} the unit matrix in color space.

C The complex scheme

In this appendix we give an algorithm to fix the renormalized parameters in the complex renormalization scheme in terms of the input parameters. We discuss two options for the input parameters, the LEP1 input-parameter scheme and the LEP2 input-parameter scheme.

As a first option we take the input parameters of the LEP1 scheme, i.e., the real LEP1 Z-boson mass m_Z, the Fermi coupling G_F, the effective electromagnetic coupling $\mathrm{Re}\{\alpha_\ell(m_Z^2)^{-1}\}$ at the LEP1 Z peak, and the top-quark mass m_t.

First we compute the bare parameters for given Δ and μ_0, where Δ is the dimensional regularized infinity in the loop corrections and μ_0 the squared mass parameter of dimensional regularization.

The bare electromagnetic coupling is calculated through the relation

$$\frac{1}{\hat{\alpha}} = \frac{1}{\alpha(p^2)} - \frac{S_\gamma(p^2, m_t^2)}{p^2}\,, \tag{74}$$

at $p^2 = m_Z^2$, where we have split the photon self-energy according to

$$\hat{\Sigma}_\gamma(p^2) \equiv \hat{\alpha}\, S_\gamma(p^2, m_t^2). \tag{75}$$

Our $\alpha(m_z^2)$ differs from the commonly used effective electromagnetic coupling $\alpha_\ell(m_z^2)$ that is extracted from the ratio $R(s) = \sigma(e^+e^- \to \text{hadrons})/\sigma(e^+e^- \to \mu^+\mu^-)$ via a dispersion relation [14]. The difference is due to the top-quark contribution to the photon self-energy, which is included in $\alpha(m_z^2)$ but not in $\alpha_\ell(m_z^2)$, where the index "ℓ" refers to "light fermions". Since both running couplings coincide at zero-momentum transfer, $\alpha(0) = \alpha_\ell(0)$, we have

$$\frac{1}{\alpha(m_z^2)} = \frac{1}{\alpha_\ell(m_z^2)} + \frac{S_{\gamma,t}(m_z^2, m_t^2)}{m_z^2} - \left.\frac{\partial S_{\gamma,t}(p^2, m_t^2)}{\partial p^2}\right|_{p^2=0} , \tag{76}$$

where $S_{\gamma,t}$ includes only the contribution of the top-quark loop of S_γ, which can be easily read off from Eq.(54).

The knowledge of $\text{Re}\{\alpha_\ell(m_z^2)^{-1}\} = 128.89 \pm 0.09$ [14] is sufficient to fix $\text{Re}\{\alpha(m_z^2)^{-1}\}$ by Eq.(76). Then the real part of Eq.(74) determines the (real) bare coupling $\hat{\alpha}$, and the imaginary part of Eq.(74) yields

$$\text{Im}\{\alpha(m_z^2)^{-1}\} = \text{Im}\,\frac{S_\gamma(m_z^2, m_t^2)}{m_z^2} , \tag{77}$$

so that also $\alpha(m_z^2)$ is completely known. As already mentioned, a precise determination of $\alpha(p^2)$ requires the knowledge of the non-perturbative hadronic part of S_γ. Given $\text{Re}\{\alpha_\ell(m_z^2)^{-1}\}$ as experimental data point, we obtain $\alpha(p^2)$ through a perturbative evolution with massless fermions (apart from the top quark) in order to match the vertex corrections which also have massless fermions and no QCD corrections. In order to test the numerical relevance of our procedure we have verified that the resulting $\alpha(p^2)$ agrees, over a wide range of p^2, to better than 0.1% with the one that has been evolved from $\alpha(0)$ through a non-perturbative parameterization of the hadronic vacuum polarization [14].

The Fermi condition is used to fix the ratio of the bare W-boson mass $\sqrt{\hat{\mu}_w}$ and the weak coupling $\hat{g}_w$, where massive fermions, i.e., in practice only the top quark, give an extra contribution:

$$2\sqrt{2}\,G_F = \frac{\hat{g}_w^2}{\hat{\mu}_w - \hat{g}_w^2\,T_w(0)} \;\longrightarrow\; \kappa \equiv \frac{\hat{g}_w^2}{\hat{\mu}_w} = \frac{2\sqrt{2}\,G_F}{1 + 2\sqrt{2}\,G_F\,T_w(0)} . \tag{78}$$

The bare W-boson mass is reconstructed by inverting the LEP1 mass-renormalization condition $\hat{\mu}_z = m_z^2 + \text{Re}\,\hat{Z}(m_z^2)$ for the Z-boson mass. Using Eq.(3), Eqs.(74–75), the decomposition

$$\hat{\overline{\Sigma}}_w(p^2) \equiv \hat{g}_w^2\,S_w(p^2, m_t^2), \tag{79}$$

and

$$\hat{g}_w^2 = \kappa\,\hat{\mu}_w, \quad \hat{s}_w^2 = 2\pi\hat{\alpha}/\hat{g}_w^2, \quad \hat{c}_w^2 = 1 - \hat{s}_w^2, \quad \hat{\mu}_z = \hat{\mu}_w/\hat{c}_w^2, \tag{80}$$

this leads to

$$A \;=\; 1 - \kappa\;\text{Re}\,T_z(m_z^2) - \kappa\,\text{Re}\left[S_w(m_z^2, m_t^2) - \frac{2\pi\,\alpha(m_z^2)\,S_w^2(m_z^2, m_t^2)}{m_z^2}\right] ,$$

$$
\begin{aligned}
B &= -m_z^2 + 4\pi\,\mathrm{Re}\Big[\alpha(m_z^2)\,S_w(m_z^2,m_t^2)\Big]\,,\\
C &= \frac{2\pi}{\kappa}\,m_z^2\,\mathrm{Re}\,\alpha(m_z^2)\,,\\
\hat{\mu}_w &= \Big[-B+\sqrt{B^2-4AC}\Big]/(2A)\,.
\end{aligned}
\tag{81}
$$

For $m_f = 0$, $f \neq t$, $S_w(m_z^2, m_t^2)$ can be replaced by $(3/16\pi)S_\gamma(m_z^2, m_t^2)$ in Eq.(81). Now from Eq.(80) all bare parameters can be computed.

At this point we choose to work in the complex renormalization scheme. The running couplings are computed using Eqs.(8–10). Using Eq.(74) for $1/\alpha(p^2)$ and a similar expression derived from Eq.(9) for $1/g_w^2(p^2)$, it can be proven that the running couplings, deduced from the input in the above way, are finite. From this the finiteness of the propagator functions and vertex functions follows. This also holds for the masses of the weak vector bosons, which are computed by iteration.

We start off the iteration by initializing the complex masses of the Z and W boson by

$$
\mu_z^{\mathrm{ini}} = m_z^2 - i m_z \Gamma_z\,, \qquad \mu_w^{\mathrm{ini}} = m_w^2 - i m_w \Gamma_w\,,
\tag{82}
$$

with m_z, Γ_z the real LEP1 Z-boson mass and width, and m_w, Γ_w reasonable estimates for the real W-boson mass and width. The iteration is based on the equations

$$
\begin{aligned}
\mu_w &= g_w^2(\mu_w)\left[\frac{1}{2\sqrt{2}\,G_F} - T_w(\mu_w) + T_w(0)\right]\,,\\
\mu_z &= \frac{g_w^2(\mu_z)}{c_w^2(\mu_z)}\left[\frac{1}{2\sqrt{2}\,G_F} - T_z(\mu_z) + T_w(0)\right]\,,
\end{aligned}
\tag{83}
$$

which follow from the complex mass-renormalization conditions Eqs.(13–14) and Eq.(78). We have verified that the iteration yields finite values for the complex masses, independent of the regularization parameters Δ and μ_0.

As a check, we applied the optical theorem to the processes $e^+\nu_e \to e^+\nu_e$ and $e^+e^- \to e^+e^-$, and verified that the computed complex gauge-boson masses satisfy the resulting relations.

For experiments at LEP2 it is more natural to use m_w as an input parameter. Following Ref. [4] this can be done by determining m_t from $\mathrm{Re}\{\alpha_\ell(m_z^2)^{-1}\}$, m_z, G_F, and m_w. The real W-boson mass m_w obeys the condition $\hat{\mu}_w = m_w^2 + \mathrm{Re}\,\hat{\Sigma}_w(m_w^2)$. Using the relations mentioned before Eq.(81) this gives

$$
\hat{\mu}_w = m_w^2\left[1 - \kappa\,\mathrm{Re}\,T_w(m_w^2) - \kappa\,\mathrm{Re}\,S_w(m_w^2, m_t^2)\right]^{-1}.
\tag{84}
$$

Equating this to $\hat{\mu}_w$ from Eq.(81) and using $\alpha(m_z^2)$ as derived from Eqs.(76–77) yields a relation between m_z, G_F, $\mathrm{Re}\{\alpha_\ell(m_z^2)^{-1}\}$, m_w, and m_t. This can be solved iteratively for m_t. The rest is done as above.

D The complex scheme versus the LEP1 scheme

In this appendix we give a short description of the perturbative relation between the complex-mass scheme and the more familiar on-shell (LEP1) scheme. We consider the unrenormalized V self-energy, $\hat{\Sigma}_V$, which contains possible tadpole contributions. If $\hat{\mu}_V$ is the bare V-boson mass squared then the complex pole μ_V is defined by

$$\mu_V - \hat{\mu}_V + \hat{\Sigma}_V(\mu_V; \hat{\mu}_V) = 0 \,. \tag{85}$$

The complex pole is a basic property of the S-matrix, and therefore gauge-invariant. Here we stress that in the full theory one should actually write $\hat{\Sigma}_V(s;\mu)$, where μ denotes the squared mass to be used in the propagators for the internal V lines. In the following the second argument of $\hat{\Sigma}_V(s;\mu)$ is omitted, since we always understand that bare masses and couplings are inserted in the loop calculations. Alternatively, one could of course insert renormalized quantities inside the loops, but then additional counter-term contributions would have to be taken into account, which become relevant at the two-loop level.

For clarity, we first develop the formalism up to and including two-loop order accuracy in the relations for the V-boson mass and width, and turn to the special case of fermionic one-loop corrections afterwards. The complex pole is rewritten in terms of real quantities $\bar{m}_V$ and $\bar{\Gamma}_V$ as

$$\mu_V = \bar{m}_V^2 - i\,\bar{\Gamma}_V \bar{m}_V \,, \tag{86}$$

so that Eq.(85) yields

$$\begin{aligned} \bar{m}_V^2 - i\,\bar{\Gamma}_V \bar{m}_V &= \hat{\mu}_V - \hat{\Sigma}_V(\bar{m}_V^2 - i\,\bar{\Gamma}_V \bar{m}_V) \\ &= \hat{\mu}_V - \hat{\Sigma}_V(\bar{m}_V^2) + i\,\bar{\Gamma}_V \bar{m}_V \hat{\Sigma}'_V(\bar{m}_V^2) + \frac{1}{2}\bar{\Gamma}_V^2 \bar{m}_V^2 \hat{\Sigma}''_V(\bar{m}_V^2) + \dots \,. \end{aligned} \tag{87}$$

Taking the real and imaginary parts of Eq.(87), we get relations for the mass,

$$\bar{m}_V^2 = \hat{\mu}_V - \mathrm{Re}\,\hat{\Sigma}_V(\bar{m}_V^2) - \bar{\Gamma}_V \bar{m}_V \,\mathrm{Im}\,\hat{\Sigma}'_V(\bar{m}_V^2) + \dots \,, \tag{88}$$

and the width,

$$\bar{\Gamma}_V \bar{m}_V = \mathrm{Im}\,\hat{\Sigma}_V(\bar{m}_V^2) - \bar{\Gamma}_V \bar{m}_V \,\mathrm{Re}\,\hat{\Sigma}'_V(\bar{m}_V^2) - \frac{1}{2}\bar{\Gamma}_V^2 \bar{m}_V^2 \,\mathrm{Im}\,\hat{\Sigma}''_V(\bar{m}_V^2) + \dots \,. \tag{89}$$

The width $\bar{\Gamma}_V$ can be eliminated from the right-hand sides of Eq.(88) and Eq.(89) by iteration,

$$\bar{m}_V^2 = \hat{\mu}_V - \mathrm{Re}\,\hat{\Sigma}_V(\bar{m}_V^2) - [\mathrm{Im}\,\hat{\Sigma}_V(\bar{m}_V^2)][\mathrm{Im}\,\hat{\Sigma}'_V(\bar{m}_V^2)] + \dots \,, \tag{90}$$

$$\begin{aligned} \bar{\Gamma}_V \bar{m}_V = \mathrm{Im}\,\hat{\Sigma}_V(\bar{m}_V^2) \Big\{ & 1 - \mathrm{Re}\,\hat{\Sigma}'_V(\bar{m}_V^2) + [\mathrm{Re}\,\hat{\Sigma}'_V(\bar{m}_V^2)]^2 \\ & - \frac{1}{2}[\mathrm{Im}\,\hat{\Sigma}_V(\bar{m}_V^2)][\mathrm{Im}\,\hat{\Sigma}''_V(\bar{m}_V^2)] \Big\} + \dots \,. \end{aligned} \tag{91}$$

We now introduce the usual on-shell mass m_V,

$$m_V^2 = \hat{\mu}_V - \mathrm{Re}\,\hat{\Sigma}_V(m_V^2)\,. \tag{92}$$

Eliminating $\hat{\mu}_V$ from Eq.(90) and Eq.(92), $\bar{m}_V^2$ can be calculated from m_V^2 by iteration

$$\bar{m}_V^2 = m_V^2 - [\mathrm{Im}\,\hat{\Sigma}_V(m_V^2)][\mathrm{Im}\,\hat{\Sigma}_V'(m_V^2)] + \dots\,, \tag{93}$$

i.e., $\bar{m}_V^2$ and m_V^2 coincide at the one-loop level, but differ by two-loop corrections. The on-shell V-boson width is defined as

$$\begin{aligned}\Gamma_V m_V &= \frac{\mathrm{Im}\,\hat{\Sigma}_V(m_V^2)}{1+\mathrm{Re}\,\hat{\Sigma}_V'(m_V^2)} \\ &= \mathrm{Im}\,\hat{\Sigma}_V(m_V^2)\Big\{1-\mathrm{Re}\,\hat{\Sigma}_V'(m_V^2)+[\mathrm{Re}\,\hat{\Sigma}_V'(m_V^2)]^2+\dots\Big\}\,,\end{aligned} \tag{94}$$

giving

$$\begin{aligned}\bar{\Gamma}_V\bar{m}_V &= \Gamma_V m_V - [\mathrm{Im}\,\hat{\Sigma}_V(m_V^2)][\mathrm{Im}\,\hat{\Sigma}_V'(m_V^2)]^2 \\ &\quad - \frac{1}{2}[\mathrm{Im}\,\hat{\Sigma}_V(m_V^2)]^2[\mathrm{Im}\,\hat{\Sigma}_V''(m_V^2)] + \dots\,.\end{aligned} \tag{95}$$

As a next step, we specialize the above formulae to fermionic one-loop corrections and to the case where the V particle decays exclusively into massless fermions. Then, we have the relations

$$\mathrm{Im}\,\hat{\Sigma}_V(s) = \frac{\Gamma_V}{m_V}s\,, \qquad \mathrm{Im}\,\hat{\Sigma}_V'(s) = \frac{\Gamma_V}{m_V}\,, \tag{96}$$

in the vicinity of $s = m_V^2$, so that Eq.(93) and Eq.(95) yield

$$\bar{m}_V^2 = m_V^2 - \Gamma_V^2 + \dots\,, \tag{97}$$

$$\frac{\bar{\Gamma}_V}{\bar{m}_V} = \frac{\Gamma_V}{m_V} + \dots \qquad \text{or} \qquad \bar{\Gamma}_V = \Gamma_V\left(1-\frac{\Gamma_V^2}{2m_V^2}\right) + \dots\,. \tag{98}$$

Equations (97-98) represent the perturbative solutions of the basic equations given in App. C and are the basis of the so-called fixed-width scheme that we have used in Section 4.

Finally we consider the V propagator, which can be rewritten as

$$\hat{P}_V(s) = [s - \hat{\mu}_V + \hat{\Sigma}_V(s)]^{-1} = [s - \mu_V + \hat{\Sigma}_V(s) - \hat{\Sigma}_V(\mu_V)]^{-1}\,. \tag{99}$$

In the vicinity of the resonance it is possible to extract the "running-width contributions" from $\hat{\Sigma}_V(s)$ according to Eq.(96) as follows,

$$\hat{\Sigma}_V(s) = \hat{\Sigma}_V^{\mathrm{rem}}(s) + i\frac{\Gamma_V}{m_V}s. \tag{100}$$

Inserting Eq.(100) into Eq.(99) and using the relations Eq.(86), Eq.(97), and Eq.(98), we arrive at

$$\hat{P}_V(s) = \left[s - m_V^2 + i\frac{\Gamma_V}{m_V}s + \hat{\Sigma}_V^{\rm rem}(s) - \hat{\Sigma}_V^{\rm rem}(\mu_V) \right]^{-1} , \tag{101}$$

showing the appearance of the familiar line-shape parameters for the process $e^+e^- \to V \to \bar{f}f$. The "remainder" $\hat{\Sigma}_V^{\rm rem}(s)$ consists of the complete real part of the self-energy $\hat{\Sigma}_V(s)$ and the contribution of heavy fermions to the imaginary part, such as the top-quark contributions for $V = W, Z$, which become relevant at $s > (m_t + m_b)^2$ and $s > 4m_t^2$, respectively. Equation (101) explicitly illustrates that all fermionic self-energy corrections are resummed.

The same translation dictionary between complex-mass scheme and on-shell scheme will work in the more realistic case where we consider the full neutral sector of the Standard Model, therefore including also γ–γ and Z–γ transitions. Owing to the photon–Z-boson mixing, the Z-boson self-energy, $\hat{\Sigma}_Z(p^2)$, is effectively replaced by $\hat{Z}(p^2)$ [see Eq.(6)].

References

[1] E.N. Argyres et al., Phys. Lett. **B358** (1995) 339.

[2] Y. Kurihara, D. Perret-Gallix and Y. Shimizu, Phys. Lett. **B349** (1995) 367.

[3] D. Bardin, W. Hollik and G. Passarino (eds.), *Reports of the working group on precision calculations for the Z resonance* (CERN 95-03, Genève, 1995).

[4] W. Beenakker et al., in *Physics at LEP2*, eds. G. Altarelli, T. Sjöstrand and F. Zwirner, (CERN 96-01, Genève, 1996) Vol. 1, p. 79, hep-ph/9602351.

[5] P.M. Zerwas (ed.), e^+e^- *collisions at 500 GeV: The physics potential* (DESY 93-123C, Hamburg, 1993);
W. Beenakker and A. Denner, Int. J. Mod. Phys. A9 (1994) 4837.

[6] A. Denner, S. Dittmaier and G. Weiglein, Nucl. Phys. **B440** (1995) 95;
A. Denner and S. Dittmaier, Phys. Rev. **D54** (1996) 4499.

[7] M. Veltman, Physica **29** (1963) 186;
R. G. Stuart, Phys. Lett. **B262** (1991) 113.

[8] W. Beenakker, G. J. van Oldenborgh, J. Hoogland and R. Kleiss, Phys.Lett. **B376** (1996) 136.

[9] A. Denner, Fortschr. Phys. **41** (1993) 307.

[10] G. 't Hooft and M. Veltman, Nucl. Phys. **B50** (1972) 318;
for our conventions see e.g. Ref. [9].

[11] D. Bardin et al., in *Physics at LEP2*, eds. G. Altarelli, T. Sjöstrand and F. Zwirner, (CERN 96-01, Genève, 1996) Vol. 2, p. 3.

[12] U. Baur and D. Zeppenfeld, Phys. Rev. Lett. **75** (1995) 1002.

[13] C. G. Papadopoulos, Phys. Lett. **B352** (1995) 144.

[14] S. Eidelman and F. Jegerlehner, Z. Phys. **C67** (1995) 585;
H. Burkhardt and B. Pietrzyk, Phys. Lett. **B356** (1995) 398.

[15] F. Abe et al., Phys. Rev. Lett. **74** (1996) 2626; and contributed paper to ICHEP96, PA-08-018;
D0 Collaboration, S. Abachi et al., contributed papers to ICHEP96, PA-05-027 and PA-05-028;
P. Grannis, talk presented at ICHEP96, to appear in the proceedings.

[16] C. Papadopoulos, ERATO: event generator for four-fermion production at LEP2 energies and beyond, hep-ph/9609320, to appear in Comp. Phys. Commun.

[17] G. Passarino, Comp. Phys. Comm. **97** (1996) 261;
G. Passarino, Acta Phys. Pol. **B27** (1996) 1605.

[18] G. J. van Oldenborgh, P. Franzini, A. Borrelli, Comp. Phys. Comm. **83** (1994) 14.

[19] M. Grünewald, private communication.

[20] J. Hoogland and G.J. van Oldenborgh, in preparation.

[21] M. Beuthe, R. Gonzalez Felipe, G. López Castro and J. Pestieau, preprint UCL-IPT-96-20, hep-ph/9611434.